The Nuclear Field Shift Effect in Chemical Exchange Reactions

Toshiyuki Fujii[a], *Frédéric Moynier*[b], *Francis Albarède*[c]

[a]Research Reactor Institute, Kyoto University, 2-1010 Asashiro Nishi, Kumatori, Sennan Osaka 590-0494, Japan

[b]Department of Earth and Planetary Sciences, Washington University in St. Louis, Campus Box 1169, 1 Brookings Drive, Saint Louis, MO 63130-4862, USA

[c]Laboratoire de Sciences de la Terre, UMR 5570 CNRS, Ecole Normale Supérieure de Lyon, 46, Allee d'Italie, 69364 Lyon Cedex 7, France

*Author to whom correspondence should be addressed

tosiyuki@rri.kyoto-u.ac.jp

TEL: +81-724-51-2469, FAX: +81-724-51-2634

Keywords: Nuclear field shift; Mass-independent; Isotope fractionation; Chemical exchange

Abstract

Mass-independent isotope fractionations found in laboratory-scale chemical exchange experiments are reviewed. The classic theory of stable isotope fractionation in chemical exchange reactions has been established by Bigeleisen, Mayer, and Urey in 1947. In 1996, the conventional mass-dependent theory was expanded by Bigeleisen to include a mass-independent term named the nuclear field shift effect. The nuclear field shift is an isotope shift in orbital electrons, which results from the isotopic difference in nuclear size and shape. Since the revised theory was proposed, the mass-independent isotope fractionation of various elements, (*e.g.*, Ti, Cr, Zn, Sr, Mo, Ru, Cd, Sn, Te, Ba, Nd, Sm, Gd, Yb, and U), found in chemical exchange systems has been successfully explained as the nuclear field shift effect. In this review article, from both theoretical and experimental viewpoints, origins of mass-independent isotope effects are discussed.

1. Introduction

This article presents an overview of the mass-independent isotope fractionation found in laboratory scale chemical exchange experiments, whose origin is considered to be the nuclear field shift effect. The fundamental theory of the chemical isotope effect was established by Urey (1947) and Bigeleisen and Mayer (1947). From the theory, at a constant temperature, the isotope enrichment factor is proportional to the isotopic mass difference δm and inversely proportional to the product of masses m and m' of two isotopes. As long as four decades after the formulation of the mass-dependent theory, a failure of the isotope effect in chemical exchange equilibria to follow the theory has not been reported.

Mass-independent isotope fractionations were first observed for O and S (see a review by Thiemens, 2006). The difference in the symmetry and the densities of states of the activated isotopomers is a possible origin for these mass-independent isotope fractionations (Hathorn and Marcus, 1999). Alternative interpretations have been discussed in review articles (Weston, 1999; Thiemens, 2006). For heavy elements, an anomalous isotope effect in chemical exchange was found in an isotope enrichment of ^{235}U in a redox reaction (Fujii et al., 1989a,b). Isotope enrichment factors for even atomic mass isotopes, ^{234}U, ^{236}U, and ^{238}U, showed a mass-dependent line, while that of ^{235}U deviated from that line. After that observation, the anomalous isotope enrichment of odd atomic mass isotopes has been examined. In cation exchange chromatography, a similar property has been found in ^{157}Gd enrichment (Chen et al., 1992), while fractionations of Ca (Oi et al., 1993), Sr (Oi et al., 1992), and Ba (Kondoh et al., 1996) isotopes showed the conventional mass-dependent trends. Nishizawa et al. (1993, 1994) have found different fractionation properties between odd and even atomic mass

isotopes of Zn (1993), Sr (1994), and Ba (1994) in a liquid-liquid extraction system with a macrocyclic polyether. The effect was named "odd/even isotope effect" (Nishizawa et al., 1994), but at that time, the origin of the odd/even isotope effect was not clear.

A further investigation on the odd/even isotope effect has been carried out for Sr isotopes (Nishizawa et al., 1995). In the study, a similarity between the odd/even isotope effect and the odd-even staggering found in atomic spectra was observed. In atomic spectra, lines of the odd isotopes do not lie midway between the adjacent even isotopes, but are shifted towards the isotope of lower atomic mass number. This effect, which is known as the odd-even staggering (Stacy, 1966; Kurn, 1969; Heilig and Steudel, 1978, King, 1984; Aufmuth et al., 1987), is attributable to their nuclear charge radii. Odd neutron number nuclei often appear to be smaller than that estimated from the adjacent even isotopes (see Fig. 3 in a review by Aufmuth et al., 1987).

In 1996, the Bigeleisen-Mayer equation was expanded by the original author (Bigeleisen, 1996a). The nuclear field shift effect, which is one of the terms added in the expansion, is recognized as the origin of the mass-independent isotope fractionation. The nuclear field shift is an isotope shift in orbital electrons (Kurn, 1969; Heilig and Steudel, 1978, King, 1984; Aufmuth et al., 1987). This results from the isotopic difference in nuclear size and shape. Different isotopes have the same number of protons, but they do not have the same distribution of protons in space. That is, the nuclear charge distribution is affected by the number of neutrons in the nucleus. The nuclear charge distribution gives an electric field, and its isotopic difference shifts the atomic energy levels (details will be explained in section, 4.1), also displacing the electronic molecular states. The nuclear field shift is not mass-dependent but is strongly

related to neutron configuration of a nuclear structure. The nuclear field shift effect is therefore a mass-independent isotope effect. The new theory gave a sufficient explanation of the anomalous isotope enrichment of U. Nomura et al. (1996) have independently come to the same conclusion. At the current stage, the Bigeleisen 1996 theory is the most reliable theory for studying the mass-independent isotope fractionation found in chemical exchange reactions.

2. Chemical exchange reaction

The theory of chemical isotope effect has been derived for equilibrium reactions based upon the calculation of the isotopic reduced partition function (Urey, 1947; Bigeleisen and Mayer, 1947). The isotopic reduced partition function based on differences in vibrational frequencies of isotopically substituted molecules is an estimate of isotopic partitioning between a separated atom and the molecule.

Chemical exchange is known as a potential method for separating isotopes (London, 1961). A chemical exchange reaction can be represented as two half-reactions,

$$AX + Y \rightleftarrows AY + X, \quad \Delta G_1^\circ \tag{1}$$

or

$$A'X + Y \rightleftarrows A'Y + X, \quad \Delta G_2^\circ \tag{2}$$

where A and A' are the heavy and light isotopes of the element A, and X and Y represent ligands. ΔG_1° and ΔG_2° are the standard free energies of the reactions. The difference between reactions 1 and 2 corresponds to an isotopic exchange reaction between AX and AY,

$$A'Y + AX \rightleftarrows A'X + AY, \quad \Delta G^\circ = \Delta G_1^\circ - \Delta G_2^\circ \tag{3}$$

For example, isotopes of light elements, C (Hutchison et al., 1940), N (Urey et al., 1937), and S (Stewart and Cohen, 1940), were successfully separated by chemical exchange in Urey's pioneering work. Even for heavy elements like U, isotope enrichment by chemical exchange is feasible (see a review by Bigeleisen, 1992).

The equilibrium constants of reactions 1 and 2 are,

$$K_1 = \frac{\gamma_{AY}[AY]\,\gamma_X[X]}{\gamma_{AX}[AX]\,\gamma_Y[Y]} \tag{4}$$

and,

$$K_2 = \frac{\gamma_{A'Y}[A'Y]\,\gamma_X[X]}{\gamma_{A'X}[A'X]\,\gamma_Y[Y]} \tag{5}$$

where γ means the activity coefficient. K_1/K_2 can be calculated as,

$$\frac{K_1}{K_2} = \frac{(\gamma_{AY}[AY])/(\gamma_{A'Y}[A'Y])}{(\gamma_{AX}[AX])/(\gamma_{A'X}[A'X])} \tag{6}$$

This is identical with the equilibrium constant K of the isotopic exchange reaction 3. From the general thermodynamic relation $\Delta G° = -RT \ln K$, a relation $\Delta G_1° - \Delta G_2° = -RT \ln K_1 - (-RT \ln K_2) = -RT \ln (K_1/K_2)$ can be obtained. Hence, the relation $K = K_1/K_2$ is thermochemically consistent.

Under the equilibrium of reaction 3, if the chemical species AX and A'X are separated from AY and A'Y, isotope fractionation can be evaluated. In the case, the equilibrium isotope separation factor α is defined as,

$$\alpha = \frac{([A]/[A'])_Y}{([A]/[A'])_X} \tag{7}$$

where $([A]/[A'])_X$ means the isotopic composition corresponding to AX and A'X, while $([A]/[A'])_Y$ corresponds to AY and A'Y. $([A]/[A'])_X$ and $([A]/[A'])_Y$ may be the isotopic

123 compositions of two different equilibrated phases, *e.g.*, an aqueous phase and an organic
124 phase in solvent extraction, a resin phase and a liquid phase in chromatography, and so
125 on. Under an assumption that the activity coefficient is isotope-independent, that is, γ_{AX}
126 = $\gamma_{A'X}$ and γ_{AY} = $\gamma_{A'Y}$ (see Eq. 6), the isotope separation factor α is equal to the
127 equilibrium constant *K* of reaction 3.

128 The isotope enrichment factor ε is defined as,

$$\varepsilon = \alpha - 1 \quad (8)$$

129 Considering the magnitude of chemical isotope fractionation, an approximation, $\alpha - 1 \approx$
130 $\ln \alpha$ (or $\varepsilon \approx \ln (1 + \varepsilon)$), can be applied. Here α and ε have been defined for a single stage
131 reaction. Since chromatography is a multistage process, α and ε values are usually
132 extracted from measurements by using equations proposed by Spedding (1955),
133 Glueckauf (1955), or Kakihana and Kanzaki (1969). It should be noted that ε here is
134 different from that usually used in geochemistry (the use of ε to indicate a fractionation
135 factor is not uncommon in environmental geochemistry). ε in Eq. 8 is as defined and
136 used for engineered isotope enrichment. One can see that 10^3 ε is similar to the delta
137 unit used in geochemistry.

138

139 **3. Bigeleisen-Mayer's (1947) theory of mass-dependent fractionation**

140 Isotope effects in chemical exchange (reaction 3) caused by intramolecular vibration has
141 been clearly explained by Bigeleisen and Mayer (1947). A review prepared by Ishida
142 (2002) is helpful for understanding it. The equilibrium constant *K* in the isotope
143 exchange reaction 3 is,

$$K = \frac{\left(\frac{s}{s'} f\right)_{\mathrm{Y}}}{\left(\frac{s}{s'} f\right)_{\mathrm{X}}} \tag{9}$$

where s is the number of identical configurations obtained by fundamental geometric operations on each molecule such as symmetry or rotation (e.g., s = 1 for HCl, 2 for O_2, 12 for CH_4), and X and Y represent ligands. The number (s/s')f is called the "reduced partition function ratio." (s/s')f is generally expressed as follows via the Bigeleisen-Mayer second-order approximation,

$$\frac{s}{s'} f = 1 + \frac{1}{24}\left(\frac{\hbar}{kT}\right)^2 \frac{\delta m}{mm'} \left\langle \nabla^2 U \right\rangle \tag{10}$$

where $\hbar$, k, and T are the Plank constant, the Boltzmann constant, and temperature, respectively. m and m' are masses of two isotopes A and A'. $\delta m/mm'$ represents ($1/m'$ – $1/m$). $\langle \nabla^2 U \rangle$ is the averaged Laplacian of the intramolecular potential. This approximation is only valid at relatively high temperature (Bigeleisen, 1947; Ishida, 2002). Consider a molecule, in which the central atom of mass m or m' is symmetrically surrounded by n identical atoms (ligands) of mass M. Equation 10 can be simply rewritten as,

$$\frac{s}{s'} f = 1 + \frac{1}{24}\left(\frac{\hbar}{kT}\right)^2 \frac{\delta m}{mm'} M\nu^2 n \tag{11}$$

where ν is the vibrational frequency (totally symmetric frequency) of the molecule. Since the second term of right hand of Eq. 11 is much smaller than unity, similar approximation like $\ln(1 + \varepsilon) \approx \varepsilon$ can be applied. From Eqs. 8, 9, and 11, and the relation $\alpha \approx K$, the isotope enrichment factor can be written as,

$$\begin{aligned}\varepsilon &= \alpha - 1 \approx \ln\alpha \approx \ln K \\ &= \ln\left(\frac{s}{s'}f\right)_Y - \ln\left(\frac{s}{s'}f\right)_X \\ &\approx \frac{1}{24}\left(\frac{\hbar}{kT}\right)^2 \frac{\delta m}{mm'}\left(M_Y \nu_Y{}^2 n_Y - M_X \nu_X{}^2 n_X\right)\end{aligned} \tag{12}$$

M, ν, and n are known values, if the related chemical species are clearly identified. Therefore, ε is a function of $\delta m/mm'$ and T^2.

The Bigeleisen-Mayer theory may be understandable by using the vibrational potential curve of a diatomic molecule (Fig. 1). The theory contains three assumptions which must be accounted for:

(1) Although the Morse potential energy curve is more realistic (see Fig. 1), the vibrational energy levels are usually approximated by the energy levels $E_n = \left(n + \frac{1}{2}\right)h\nu$ (n = 0, 1, ...) of a harmonic oscillator, in which $\nu = \frac{1}{2\pi}\sqrt{\frac{\kappa}{\mu}}$, with κ being the force constant and μ the reduced mass of the molecule.

(2) Because it is acting between the electrons orbiting each atom of the molecule, the force constant κ of isotopologues is isotope-independent (for the definition of "isotopolog", see (Minkin, 1999). Hence, the harmonic potential curve is the same for all isotopologues, and only the permissible energy levels, including the zero point energy (n = 0) are isotope-dependent.

(3) The minimum value of the potential energy of isotopologues is isotope-independent. It is convenient to assume $\delta E°$ in Fig. 1 is zero.

These assumptions lead to correction terms. Especially, assumption (3) leads to a major correction. The assumption (3) means that no isotope fractionation occurs via the

electronic partition function Q_e, but $\delta E°$ (Fig. 1) has a significant value which changes Q_e. A correction term for the assumption (3) is the origin of mass-independent isotope effect named the nuclear field shift effect.

4. Bigeleisen's (1996) theory

Bigeleisen (1996a) has improved the Bigeleisen-Mayer equation by adding correction terms. The correction terms mainly result from isotope shifts in electronic molecular energy states. Knowledge of isotope shifts in atomic and molecular spectra is helpful to understand the theory.

4.1. Isotope shifts in atomic spectra

Evidence of energy quantization comes from the observation that the frequencies of radiation absorbed or emitted by atoms and molecules depend on the isotope. The differences resulting from the substitution of an isotope by another are called "isotope shifts". Isotope shifts are best known for atomic spectra, and therefore will be the main focus of this section. A number of detailed reviews (Breit, 1958, Stacy, 1966; Kurn, 1969; Heilig and Steudel, 1978, Aufmuth et al., 1987) and books (King, 1984; Fricke and Heilig, 2004) covering various aspects of isotope shifts have appeared over the past fifty years. In this section, only the basic principles will be reviewed.

Each atomic energy level is characterized by an eigenfunction of the Schrödinger equation. The associated eigenvalues define the angular momentum and the energy of this level. Mass differences between isotopes lead to shifts in the atomic energy level, because the orbital angular momentum remains the same. This isotope shift is called the mass shift. Since the nucleus is much heavier than an electron, it

moves relatively slowly and is usually approximately treated as stationary: this is the Born-Oppenheimer approximation. For light nuclides, however, the movement of the nucleus can no longer be neglected and its movement around the center of the gravity of the nucleus-electrons ensemble creates a kinetic momentum. Each orbital electron receives an excess kinetic momentum via the movement of the nucleus. The kinetic momentum is a function of mass. The isotopic difference in the mass of the nucleus results in the mass shift in atomic energy levels. One can regard the mass shift as a correction to the Born-Oppenheimer approximation. The mass shift is the sum of the normal mass shift and the specific mass shift. The normal mass shift can be calculated under the assumption that the electron wave functions are uncorrelated. The specific mass shift considers the correlation between the electron wave functions. The mass shift is proportional to the isotopic mass difference δm and inversely proportional to the product of masses m and m' of two isotopes ($\propto \delta m/mm'$).

Another isotope shift accounts for the deviation of nuclear charge distribution from a point-charge distribution. It is called the field shift and is important because the atomic energy depends upon the size and shape of the electric charge distribution of the nucleus. In general, the field shift is smaller than the mass shift for light elements, but for heavy elements, it is relatively large compared to the mass shift (see Fig. 1 reported by Stern and Snavely, 1976). As mentioned above, the nuclear charge distribution gives rise to an electric field, and differences in nuclear charge radius associated with the number of neutrons shift the atomic energy levels. Consider the electrostatic interaction between the orbital electrons and the nucleus. Electrostatic potentials of nuclei are shown in Fig. 2. Away from the nuclear region, the electric field of the nucleus can be represented as a Coulomb potential identical for all isotopes. Within the nuclear region,

it is isotopically different. For example, since the wave functions of the *s*-electrons do not go to zero next to a finite size nucleus, the effect depends on the isotope. A larger nuclear charge distribution gives a smaller binding potential than a point-charge distribution. The field shift in an atomic energy level (δE_{fs}) can be shown to be (King, 1984),

$$\delta E_{fs} = \pi |\psi(0)|^2 \frac{a_0^3}{Z} f(Z)\, \delta\langle r^2 \rangle \tag{13}$$

where $|\Psi(0)|^2$ is the electron density at the nucleus. a_0 means the Bohr radius. $f(Z)$ is a known function for each element of atomic number Z. $\delta\langle r^2 \rangle$ means the isotopic difference in the mean-square charge radius ($= \langle r^2 \rangle_A - \langle r^2 \rangle_{A'}$). From Eq. 13, it is clear that the field shift is proportional to $\delta\langle r^2 \rangle$. Due to the systematics of neutron configuration, $\langle r^2 \rangle$ shows odd-even staggering (a "saw-tooth" figure), and the nucleus is particularly compact with magic number neutrons (20, 28, 50, 82, and 126) (see Fig. 3 in a review by Aufmuth et al., 1987).

It is known that a change in the shape of a nucleus can also give rise to a field shift, even if the actual volume of the nuclear charge distribution does not change. $\delta\langle r^2 \rangle$ obtained from isotope shifts includes information of both the nuclear size and the nuclear shape. For a non-spherical charge distribution, the second-degree deformation is accounted for by a quadrupole term with axial symmetry, and the mean-square charge radius becomes (Heilig and Steudel, 1978),

$$\langle r^2 \rangle \approx \frac{3}{5} r_0 \left(1 + \frac{5}{4\pi} \langle \beta^2 \rangle \right) \tag{14}$$

where r_0 is the equilibrium charge radius of the drop (liquid-drop model) and $\langle \beta^2 \rangle$ the

mean-square quadrupole deformation parameter. This parameter can be obtained from the reduced nuclear transition probability of nuclear $0^+ \rightarrow 2^+$ transition, $B(E2, 0^+ \rightarrow 2^+)$.

$$<\beta^2> = B(E2, 0^+ \rightarrow 2^+)\left(\frac{3Zr^2}{4\pi}\right)^{-2} \tag{15}$$

with $r = 1.2\ A^{1/3}$ fm, where Z and A are the element number and the mass number, respectively. For the neutron-rich even isotopes of Nd, Sm, and Gd, the $<\beta^2>$ values show drastic changes with the atomic mass number, which suggests that, in these cases, the changes in the nuclear shape have more effect on $<r^2>$ than change in the nuclear size (King, 1984) (for example, ^{150}Sm, ^{152}Sm, and ^{154}Sm).

The total angular momentum must be conserved during a reaction. Protons, neutrons, and electrons are fermions with spins of $\pm\frac{1}{2}$. For nuclides with even numbers of protons and neutrons, *i.e.*, with integer nuclear spin, there is no spin effect. In other cases, and in particular for nuclides of odd masses, the spin of unpaired protons and neutrons interact with the orbital momentum of the electrons (Herzberg, 1944). The total angular momentum F is the resultant of the coupling of the nuclear spin I with the total angular momentum of electrons J. The corresponding quantum number F can take values,

$$F = J + I, J + I - 1, J + I - 2, \cdots, |J - I| \tag{16}$$

This gives $2J + 1$ or $2I + 1$ different values depending on whether ($J < I$) or ($J > I$). Consequently, a small energy difference between states with different F exists. Since the magnetic moment of the nucleus is smaller (by approximately a factor of 2,000) than that of the electron, the energy differences are very small. The spectrum shift due to the coupling between J and I is referred to as the "hyperfine structure" or "hyperfine

splitting."

In a magnetic field, a space quantization of F takes place. The quantum number M_F of the component of the angular momentum in the field direction can take,

$$M_F = F\ , F-1, F-2, \cdots, -F \tag{17}$$

The $2F + 1$ values of M_F correspond to states of different energies in a magnetic field. In the absence of the magnetic field, these energy levels are degenerated to be unity. Under a strong magnetic field, these levels are split. This effect is called the Zeeman effect (for example, Fig. VI, 12 in the book by Kuhn, 1969). In general, a field of 20,000 G is needed to produce a splitting of about 1 cm^{-1} (Atkins, 1998).

A space quantization of total angular momentum F also takes place in electric fields and the $2F + 1$ levels are also split. All splitting levels are doublets ($\pm M_F$) except for $M_F = 0$ (singlet). This effect is called the Stark effect (Herzberg, 1944; Atkins, 1998).

Except for strong electromagnetic fields, the hyperfine splitting shifts due to the *I*-*J* coupling can be predicted. In order to calculate the hyperfine structure, the centroid of the energy levels must be calculated. If the energy reference level is set to be zero, the condition is,

$$\Sigma\, N_{\mathrm{i}} \Delta E_{\mathrm{i}} = 0 \tag{18}$$

where N_{i} is the occupation number of ith hyperfine splitting level and ΔE_{i} is the energy difference from the energy gravity. The value of N_{i} for each hyperfine splitting level can then be calculated as,

$$N_{\mathrm{i}} = \frac{2F_i + 1}{\sum(2F+1)} \tag{19}$$

288

289 *4.2. Outline of the Bigeleisen's (1996) theory of nuclear field shift effect*

290 Bigeleisen (1996a) expanded his original mass-dependent theory of reduced partition
291 functions (Bigeleisen and Mayer, 1947), and therefore of isotope separation factor α,
292 by adding correction terms. The isotope enrichment factor ε ($\approx \ln \alpha$) is,

$$\ln \alpha = \ln \alpha_0 + \ln K_{anh} + \ln K_{BOELE} + \ln K_{hf} + \ln K_{fs} \quad (20)$$

293 where $\ln \alpha_0$ is the Bigeleisen-Mayer equation (Eq. 12). The correction terms are

294 • the anharmonic vibration correction (K_{anh})

295 • the correction to the Born-Oppenheimer approximation (K_{BOELE})

296 • the nuclear spin effect (K_{hf}), and

297 • the nuclear field shift effect (K_{fs}).

298 The anharmonic correction is in the order of 1% of $\ln \alpha_0$ even for $^2H/^1H$ exchange
299 reactions (Bigeleisen, 1996a). Even if the potential energy curve (Fig. 1) is treated as
300 the Morse type or the typical parabola type, the difference is insignificant.

301 All the correction terms K_{BOELE}, K_{fs}, and K_{hf}, originate from the isotopic
302 displacement of the molecular energy state. They are attributable to the mass shift, the
303 field shift, and the hyperfine splitting shift, respectively. In other words, they are
304 attributable to the isotopic differences in the nuclear mass, the nuclear size and shape,
305 and the nuclear spin, respectively. In Fig. 1, the isotope separation factor due to $\delta E°$
306 corresponds to these terms and can be shown to be a ratio of electronic partition
307 functions,

$$\alpha(\delta E°) = \frac{(Q_e / Q_e')_Y}{(Q_e / Q_e')_X} = \frac{e^{-\delta E_Y^\circ / kT}}{e^{-\delta E_X^\circ / kT}} \quad (21)$$

The isotope enrichment factor is,

$$\varepsilon(\delta E^\circ) \approx \ln \alpha(\delta E^\circ) = \frac{1}{kT}\left(\delta E_X^\circ - \delta E_Y^\circ\right) \tag{22}$$

On a spectroscopic basis, δE° can be replaced by $h\nu$, where ν stands for the frequency of isotope shift in wavenumbers. The magnitude of isotope fractionation may be predicted by substituting the value of optical isotope shifts into Eq. 22, though it is based on an assumption that the minimums of potential curves have similar isotopic displacements.

The correction to the Born-Oppenheimer approximation has been investigated by Kleinman and Wolfsberg (1973 and 1974a,b). The K_{BOELE} value has been estimated for a reaction involving uranium isotopologues, in which it was concluded that the correction due to this term was negligible (Bigeleisen, 1996a). Considering the predominance of mass shift in isotope shifts, K_{BOELE} for lighter elements should be more important. The effect is however mass-dependent. The correction term K_{hf} for uranium has been calculated to be negligibly small (Bigeleisen, 1996a).

4.3. Comments on the nuclear spin effect

Let us now re-assess the reasons why Bigeleisen (1996a) concluded the nuclear spin effect be negligible. The data used are the hyperfine splitting shifts obtained from the electron magnetic resonance analysis of a ^{235}U(III) complex and are shown in Fig. 3. The ΔE_{i} values were equated to the energy differences of hyperfine splitting levels of ^{235}U with respect to the ground energy level of the ^{238}U(III) complex. As discussed in the previous section, the Stark effect must be considered for the case of a strong electromagnetic field. In this case, the occupation number of each state is not the usual

330 case of Eq. 19, but,

$$N_i = \frac{g_i}{\sum g} \tag{23}$$

331 where g_i is the degeneracy (2 for doublet and 1 for singlet) of the *i*th hyperfine splitting
332 level. If the mean weighted value of the hyperfine splitting levels is defined as the
333 reference level, the following relation is obtained,

$$\Sigma\, g_i(\Delta E_i - \delta\Delta E) = 0 \tag{24}$$

334 where $\delta\Delta E$ means the difference of the energy gravity from the ^{238}U ground energy state.
335 This equation is similar to Eq. 18. Since ΔE_i here is the energy difference from the ^{238}U
336 ground energy state, $\delta\Delta E$ must be subtracted from ΔE_i. The literature value of $\delta\Delta E$
337 (Table 2, Bigeleisen, 1996a) is only of 0.003 cm^{-1}, *i.e.*, about 10 times smaller than the
338 largest ΔE_i (see Table 2, Bigeleisen, 1996a)). The partition function of the nuclear spin
339 effect was defined by Bigeleisen (1996a) as,

$$Q_{ns}\, g = \sum g_i e^{-\frac{\Delta E_i}{kT}} \tag{25}$$

340 Since the $exp(-\Delta E_i/kT)$ value is very close to unity, the following approximation
341 $exp(-\Delta E_i/kT) \approx 1 - \Delta E_i/kT$ holds, and so Eq. 25 may then be rewritten as,

$$Q_{ns}\, g \approx \sum g_i \left(1 - \frac{\Delta E_i}{kT}\right) \tag{26}$$

342 The $\Delta E_i/kT$ value is much smaller than the magnitude of g. This equation suggests that
343 the $\Delta E_i/kT$ term, which accounts for the nuclear spin effect, only changes g by a factor
344 very close to unity. Equation 26 can now be rewritten,

$$Q_{ns}\, g \approx \sum g_i - \frac{1}{kT}\sum g_i \Delta E_i \tag{27}$$

In Eq. 24, if $\delta\Delta E << \Delta E_i$, the approximation $\Sigma\, g_i \Delta E_i \approx 0$ holds and changes Eq. 27 into $Q_{ns}\, g \approx \Sigma\, g_i$, which indicates that, within the approximation of this calculation, the nuclear spin effect can be neglected.

According to the definition by Bigeleisen (1996a), the magnitude of the nuclear spin effect ($\ln K_{hf}$) should decrease with decreasing $\delta\Delta E$. A very small nuclear spin effect of ^{235}U therefore only reflects that the value of $\delta\Delta E$ used was very small. The magnitude of $\delta\Delta E$ is therefore much more important than the number and spacing of the hyperfine splitting levels. $\delta\Delta E$ refers to the same quantity as $\delta E°$ in both Eqs. 21 and 22 (and Fig. 1). Since $\delta E°$ corresponds to the energy term in K_{BOELE} and K_{fs}, $\ln K_{hf}$ may actually not reflect the nuclear spin effect only. The definition and treatment of the nuclear spin effect in the Bigeleisen 1996 theory is therefore still problematic.

The possible origin of the mass-independent isotope effect has been identified to be the nuclear field shift. The final equation in Bigeleisen's (1996a) theory is hence obtained by adding Eq. 22 (corresponding to the field shift) to Eq. 12.

$$\ln \alpha = \frac{h}{kT} \nu_{fs}\, a + \frac{1}{24}\left(\frac{\hbar}{kT}\right)^2 \frac{\delta m}{mm'}\, b \qquad (28)$$

where a is the field shift scaling factor and b is the scaling factor for the conventional mass effect (strictly, the mean Laplacian of the intramolecular potential). The first term is the mass-independent term named the nuclear field shift effect.

Though three assumptions have been adopted in the Bigeleisen-Mayer theory (see section, 3), the consequences of assumptions (1) (harmonicity) and (3) (minimum of potential energy) were clarified as the correction terms in the Bigeleisen's (1996) theory. For the assumption (2), later, it has been identified as a second-order correction

366 to the nuclear field shift (Bigeleisen, 1998).

367

368 *4.4. Second-order correction to the nuclear field shift effect.*

369 A breakdown of the assumption (2) due to wavefunctions of bonding electrons
370 being disturbed by the nuclear charge distribution has been pointed out by Nishizawa et
371 al. (1995). This idea has come from the studies on field shifts in molecular spectra
372 (Tiemann et al., 1982; Schlembach and Tiemann, 1982). In the Bigeleisen 1996 theory,
373 the nuclear field shift effect in the electronic partition function has been focused, but not
374 in the vibrational partition function.

375 The vibrational frequency of the molecule can be simply written,

$$\nu = \frac{1}{2\pi}\sqrt{\frac{\kappa}{\mu}} \tag{29}$$

376 where κ and μ are the force constant and the reduced mass, respectively. In the classic
377 theory, only the isotopic difference in μ has been treated based on the assumption that κ
378 is isotope-independent (see Assumption (2) in Chapter 3). Due to the field shift, κ
379 should have an isotopic difference δκ, which is proportional to $\delta\langle r^2\rangle$. This has been
380 theoretically and experimentally proven by Schlembach and Tiemann (1982). If δκ is
381 introduced, the logarithm of Eq. 11 can be rewritten as (Fujii et al, 2000, 2001a),

$$\ln\left(\frac{s}{s'}\right)f = \frac{1}{24}\left(\frac{\hbar}{kT}\right)^2\frac{\delta m}{mm'}M\nu^2 n + \frac{1}{24}\left(\frac{\hbar}{kT}\right)^2\left(\frac{1}{m}+\frac{1}{M}\right)\delta\kappa n \tag{30}$$

382 The question is whether the magnitude of δκ is significant or not. Bigeleisen (1998) has
383 estimated the nuclear field shift effect in the vibrational partition function for a Pb
384 isotopologue. The magnitude was 0.3% of the $\ln(s/s')f$, and hence, the effect has been
385 concluded to be only a second-order correction to the Bigeleisen-Mayer equation.

First-principles calculations, which allow for the isotopic difference in the nuclear volume, result in a very small difference in the bond lengths of Hg isotopologues (Schauble, 2007). The results support the view that these isotopic effects can be treated as a second-order correction to the nuclear field shift effect (Bigeleisen, 1998).

4.5. Experimental and theoretical approaches

There are two effective ways to examine experimental results by employing Eq. 28. The first way is graphically shown in Fig. 4. This evaluation method needs isotopes whose $\langle r^2 \rangle$'s have mass-independent characteristics. Prominent mass-independent properties are shown in the plots of $\delta\langle r^2 \rangle$ *vs* $\delta m/mm'$ for Ca, Cr, Ba, and Ce (Figs. 5 b, d, m, and n), whereas the relation for some elements (for example, Fe, Fig. 5e) shows a mass-dependent trend.

At a constant temperature, Eq. 28 can be simplified as,

$$\ln \alpha = \delta\langle r^2 \rangle A + \frac{\delta m}{mm'} B \qquad (31)$$

where A and B are scaling factors for the nuclear field shift effect and the mass effect, respectively. The isotope enrichment factors obtained experimentally are plotted as a function of $\delta m/mm'$. If the plots are linear, the nuclear field shift cannot be separated from other mass-dependent fractionation effects, which often reflects that $\delta\langle r^2 \rangle$ varies linearly with $\delta m/mm'$ (see Fig. 5e). Deviation from linearity indicates, however, a mass-independent component which is most easily accounted for by the nuclear field shift effect. If the element has three or more isotopes, the scaling factors A and B can be

408 analyzed by fitting Eq. 31 to the experimental results. Because Eq. 31 can be arbitrarily
409 fitted to any three isotope systems, unambiguous demonstration of a nuclear field shift
410 effect requires four or more isotopes (at least three even atomic mass isotopes and one
411 odd atomic mass isotope). Deviation of experimental values from the predicted values at
412 odd atomic mass isotopes may signal a nuclear spin effect. The case for nuclear field
413 shift isotope effects can be strengthened if the fit succeeds in reproducing two
414 characteristics that coexist in some elements with a number of neutrons or protons close
415 to those of a full-shell (magic numbers), the odd-even staggering and the non-linear
416 variation of the $\delta\langle r^2\rangle$ of even isotopes with respect to $\delta m/mm'$. Elements that best fulfill
417 these conditions may be Ca, Cr, Ba, and so on, which have isotopes with magic number
418 of neutron.

419 After separating the mass-dependent and the mass-independent components,
420 the validity of the magnitude of each component can be checked. The isotope
421 enrichment factor of the conventional isotope effect can be calculated by employing the
422 Bigeleisen-Mayer equation (1947). The interatomic vibrational frequencies required for
423 the calculation can be obtained from spectrophotometry (Raman and IR) or from
424 electronic structure calculations. K_{BOELE} for some isotopologues can be estimated from
425 literature data (Kleinman and Wolfsberg, 1973 and 1974a,b). A simplified calculation
426 employed for uranium (Bigeleisen, 1996a), may also be effective to predict the
427 magnitude of K_{BOELE}. In recent quantum chemical calculations, magnitudes of the
428 nuclear field shift effect have been estimated for some simple molecules or ions
429 (Schauble, 2007; Abe et al., 2008a,b).

430 The second way is graphically shown in Fig. 6. At various temperatures, Eq. 28
431 may be simplified as,

$$\ln \alpha = \frac{1}{T} C + \frac{1}{T^2} D \qquad (32)$$

where C and D are scaling factors. The C/T term represents the nuclear field shift effect and the D/T^2 term the conventional mass effect. The nuclear field shift fractionation is largest at low temperatures, but tends to dominate the total fractionation at high temperature. In cases where mass-dependent and nuclear-volume fractionation act in opposite directions, there will be a maximum (or minimum) in the total fractionation factor at some finite nonzero temperature (see Fig. 6). This evaluation method has been applied by Nomura et al. (1996) and Bigeleisen (1996b). This method works for two or more isotope systems. Whether the $<r^2>$'s of isotopes have a mass-independent trend or not, the method can be used effectively.

However, this evaluation method involves some difficulties. From the experimental standpoint, experimental temperature range is typically very limited. The curve is thus analyzed with data within a limited $1/T$ region. The extraction further presumes that the coordination number and/or complexation affinities of the relevant element or ion should stay the same over the sampled range of temperature. A difficulty of this evaluation method was pointed out in a study on Ba isotope fractionation (Shibahara et al., 2002a). An issue is that the correction term corresponding to a departure from the Born-Oppenheimer approximation, $\ln K_{\mathrm{BOELE}}$, also varies as $1/T$. If this effect cannot be neglected, the C/T term includes both mass-dependent and mass-independent components. At low temperatures and/or when the vibrational energy is high compared to the thermal energy, the isotope enrichment factor becomes proportional to $1/T$, not to $1/T^2$ (see a review by Ishida, 2002). This also interferes with the C/T term. Furthermore, mass-independent fractionation seems to be more

454 pronounced within a specific temperature range (Kotaka et al., 1992). One can select
455 the evaluation methods on the basis of the advantages and disadvantages for each of
456 them.
457
458 **5. Kinetic effects**
459 Isotope fractionation may result from isotope-dependent reaction rates (*e.g.*, formation
460 and decomposition reactions by thermally, photochemically, or electronically activated
461 reactions). The symmetry and the densities of states of the activated isotopologues may
462 be different (Hathorn and Marcus, 1999). Alternative interpretations have been
463 discussed in review articles (Weston, 1999; Thiemens, 2006).
464 Let us first briefly present a mechanism that involves nuclear field shift in
465 reaction kinetics. For an isotope exchange reaction (such as the reaction 3), let us
466 assume that there exists a transition state which controls the reaction rate and write the
467 reaction;

$$AX + Y \rightleftarrows (AXY)^{\neq} \rightarrow AY + X \tag{33}$$

468 in which the suffix ≠ stands for the transition state. The potential curve of this reaction
469 can be shown as Fig. 7. The isotopic ratio of reaction rate constants can be written,

$$\frac{k}{k'} = \frac{P}{P'}\frac{(Q/Q')_{\neq}}{(Q/Q')_{X}} \tag{34}$$

470 in which P stands for the transmission coefficient. This is a correction coefficient in the
471 transition state theory, which corrects the one-dimensional model. The partition function
472 in Eq. 34 includes the electronic partition function as well as that for the equilibrium
473 system. As shown in Fig. 7, $\delta E°$ causes an isotope effect, in which the nuclear field shift
474 effect exists and is predominant for heavy elements. If the magnitude of

mass-independent isotope fractionation found in a kinetic system is comparable with that of the equilibrium system, and if its mass-independent property is similar to the $\delta\langle r^2\rangle$ trend, then it might be affected by the nuclear field shift. If a reaction is brought to its end before equilibrium, the isotope fractionation may be affected by the kinetic isotope effect which then would also include the nuclear field shift.

The nuclear spin effect in radical reactions is known as the kinetic isotope effect (Lawler and Evans, 1971; Buchachenko, 1977) and is referred to as the "magnetic isotope effect." It reflects a magnetic field effect on the spin of excited molecules or radical pairs, e.g., photolysis of dibenzyl ketone. The rates of reaction between radical pairs are changed, not by the difference in isotopic mass, but by the hyperfine interaction between electronic and nuclear spins. The strongest magnetic isotope effects are expected for light elements like C and O, but the magnitude decreases with the atomic number. This is because the spin-orbit interaction of heavier atoms, which enhances the spin conversion of radical pairs, is insensitive to external magnetic field. Nonetheless, magnetic isotope effects have also been described for heavier elements, *i.e.*, S (Step et al., 1992), Ge (Wakasa et al., 1993, 1998), Hg (Bergquist and Blum, 2007), and U (Rykov, 1992; Buchachenko, 1995). Since radical reactions are often the hallmark of irreversible reactions, the magnetic isotope effect is different from the nuclear spin effect in equilibrium systems. If an odd/even isotope effect is found in an equilibrium system with a radical reaction, the possibility of a magnetic isotope effect nevertheless should be evaluated. The detailed mechanism of the magnetic isotope effects in radical reactions have been reviewed elsewhere (Turro, 1983; Khudyakov et al., 1993; Buchachenko, 1995, 2000, 2009; Salikhov, 1996).

6. Mass-independent isotope fractionations found in laboratory-scale chemical exchange experiments

In this section, we summarize measured mass-independent isotope fractionations element by element. We focus on the first evaluation method, described in section 4.5 and involving a plot of fractionation factors *vs* $\delta\langle r^2\rangle$. For this reason, we focus on elements which have four or more isotopes. We assume that the isotope exchange reactions in ligand exchange systems and redox systems are equilibrium processes, neglecting kinetic effects (the isotopic equilibrium has been demonstrated in pioneering studies, Jepson and Cairns, 1979; Nishizawa et al., 1984). Mass-independent isotope fractionations found in laboratory-scale chemical exchange experiments are listed in Table 1. Relevant nuclear data can be found in reviews by Aufmuth et al. (1987) King (1984), and Fricke and Heilig (2004).

6.1. Sulfur

Sulfur is the lightest of the elements which have four naturally occurring isotopes (^{32}S, ^{33}S, ^{34}S, and ^{36}S). Mass-independent isotope fractionation of S has been studied in both terrestrial and extra terrestrial samples (Farquhar et al., 2000, Thiemens, 2006). Photochemical reactions as an origin of the mass-independent isotope fractionation have been discussed. Mass-independent isotope fractionation of ^{33}S has also been found (Watanabe et al., 2007, 2009) in recent laboratory experiments (a kinetic redox reaction). On the other hand, mass-independent isotope fractionations have not yet been found in equilibrium chemical exchange systems. Because S is a moderately light element, the contribution of the nuclear field shift effect may be much smaller than the mass effect (Rai and Thiemens, 2007). According to quantum chemical calculations (Schauble,

523 2007), the nuclear field shift effect of S has been estimated to be ~0.02‰ for an even
524 atomic mass isotope pair, ^{32}S-^{36}S. Unfortunately, $<r^2>$ is not yet known for ^{33}S (Fricke
525 and Heilig, 2004) (Fig. 5a). A possibility of the odd-even staggering in S isotope
526 fractionation still remains, but it may be very small (Schauble, 2007).
527
528 *6.2. Calcium*
529 Calcium is the lightest element known to have very clear mass-independent features in
530 its nuclear charge radii. ^{40}Ca (the most abundant) and ^{48}Ca are doubly magic, *i.e.*, they
531 have full shells of both neutrons and protons (Fig. 5b). Therefore, the $<r^2>$'s of these
532 two isotopes are the smallest of all stable Ca isotopes. Calcium may therefore be one of
533 the best choices to investigate the nuclear field shift effect in very light elements.
534 Though there are several reports on chemical isotope fractionation of Ca (for
535 example, see a review by Heumann,1985), most of the data concern two isotopes only
536 (^{40}Ca and ^{44}Ca). Other early reports deal with three isotopes (^{40}Ca, ^{44}Ca, and ^{48}Ca)
537 (Heumann and Schiefer, 1980,1982; Jepson and Shockey, 1984), but the results show
538 the typical mass-dependent pattern. In a three isotope system, a mass-independent
539 isotope fractionation can be seen in some samples (*e.g.*, sample numbers 18 to 25,
540 Heumann et al., 1982). Because only three isotopes were analyzed, the nuclear field
541 shift effect cannot be unambiguously established.
542 Fujii et al. (1985) and Oi et al. (1993) have studied Ca isotope fractionations
543 with five isotopes (^{40}Ca, ^{42}Ca, ^{43}Ca, ^{44}Ca, and ^{48}Ca). Though the results were discussed
544 in the context of mass-dependent fractionation, the isotope enrichment factors show
545 some mass-independent isotope effects. In addition to odd-even staggering (Fig. 8), a
546 mass-independent fractionation pattern is observed at even atomic masses. We

547 reanalyzed these data by employing Eq. 31 (Fig. 8). Our calculations reproduce the
548 observed results well. Even though the precision of the experimental data makes the
549 discussion of mass-independent isotope fractionation tentative, the nuclear field shift
550 effect accounts well for the apparent mass-independent component.
551
552 *6.3. Titanium*
553 Titanium has five naturally occurring isotopes (^{46}Ti, ^{47}Ti, ^{48}Ti, ^{49}Ti, and ^{50}Ti). The $\langle r^2 \rangle$'s
554 of Ti show significant odd-even staggering. Ti isotopes of Ti(III) or Ti(IV) were
555 fractionated by a liquid-liquid extraction system using a crown ether (Fujii et al., 1998a)
556 (Fig. 9). A difference of isotope fractionation factors between Ti(III) and Ti(VI) systems
557 may be due to the lack of 3*d* electrons of Ti(IV), while Ti(III) possesses a single 3*d*
558 electron. Isotope enrichment factors show odd-even staggering (Fig 5c). The pattern of
559 mass-independent isotope fractionation is largely consistent with the nuclear field shift.
560 Isotope effects have also been found for odd atomic mass isotopes (^{47}Ti and ^{49}Ti). In
561 addition to nuclear spin effects, the degeneracy of the hyperfine structure of the
562 electronic partition function was considered by the authors.
563
564 *6.4. Chromium*
565 Chromium has four stable isotopes (^{50}Cr, ^{52}Cr, ^{53}Cr, and ^{54}Cr). ^{52}Cr has a closed nuclear
566 shell with 28 neutrons, which makes the nucleus of ^{52}Cr very compact and stable. The
567 $\langle r^2 \rangle$ pattern for Cr isotopes is shown in Fig. 5d. If the mass effect is minimized by
568 changing experimental conditions, the isotope enrichment factor should show same
569 trend.
570 Isotope fractionation was first investigated by solvent extraction using a crown

ether (Kawashiro et al., 1998). Observed isotope enrichment factors follow the nuclear charge radii. Subsequent studies explored different experimental and analytical conditions (Fujii et al., 2002). MC-TIMS techniques employing a total evaporation method seem to be able to minimize instrumental bias (Fujii et al., 2006a). Fujii et al. (2007, 2008a) also used MC-ICP-MS, which has been shown yield reliable, high-precision Cr isotope compositions (Yin et al., 2007; Moynier et al., 2007a), but a reliable estimate of ^{54}Cr fractionation was not provided. Isotope enrichment factors are not strictly mass-dependent and are strongly suggestive of a substantial nuclear field shift effect. Fujii et al. (2008b) repeated extractions, and calculated the isotopic mass balance between the two phases to strengthen the evidence of mass-independent isotope effects (Fig. 10).

Isotope fractionation of Cr was also investigated at high temperatures (723~1023K) by contacting a molten salt ($CrCl_3$) and a liquid metal, a redox couple Cr^0-Cr(III). The magnitude of isotope fractionation in this experiment was under the detection limit of MC-TIMS (Fujii et al, 2006a), but could be identified by MC-ICP-MS (Fujii et al., 2007). The mass-independent isotope fractionation associated with this high temperature redox reaction is consistent with a nuclear field shift effect. This would be correlated with the presence or absence of a 4*s* electron in the redox system.

6.5 Iron

There is no evidence of the mass-independent isotope fractionation of Fe (^{54}Fe, ^{56}Fe, ^{57}Fe, and ^{58}Fe) (see a review by Dauphas and Rouxel, 2006). A simple explanation is that $\langle r^2 \rangle$ is nearly linearly with mass (Fricke and Heilig, 2004) (see Fig. 5e). Even with a high precision analysis (Fujii et al., 2006b), the method based on Eq. 31 cannot

595 identify any mass-independent isotope effects (Fig. 11). The method based on Eq. 32
596 might be more suitable for Fe isotopes, but the relevant data are still missing.
597
598 *6.6. Nickel*
599 Nickel has five naturally occurring isotopes (^{58}Ni, ^{60}Ni, ^{61}Ni, ^{62}Ni, and ^{64}Ni). The $\langle r^2 \rangle$'s
600 of Ni also show only subtle odd-even staggering (Fig. 5f). Ni isotopes were fractionated
601 by a liquid-liquid extraction system by Nishizawa et al. (1997). Isotope enrichment
602 factors show an odd-even staggering trend, but the experimental errors are quite large.
603 These experiments should be re-examined in view of the recent high precision Ni
604 isotopic data acquired by MC-ICP-MS (Dauphas et al., 2008; Moynier et al., 2007b,
605 Quitté et al., 2007; Bizzarro et al. 2007; Regelous et al., 2008).
606
607 *6.7. Zinc*
608 Zinc has five naturally occurring isotopes (^{64}Zn, ^{66}Zn, ^{67}Zn, ^{68}Zn, and ^{70}Zn). Their
609 charge radii show a clear odd-even staggering (Fig. 5g). Mass-independent isotope
610 fractionation was first observed for ^{67}Zn in a chemical exchange reaction using crown
611 ether (Nishizawa et al., 1993). These early isotopic analyses were performed on an ICP
612 quadrupole mass spectrometer at rather low precision, but were later confirmed on
613 TIMS by Nishizawa et al. (1996, 1998a). The most recent investigations used
614 MC-ICP-MS (Nishizawa et al, 1998b; Fujii et al., 2001a). Because of an isotopic
615 interference of the ^{64}Ni^{+} beam, presumably emitted by the sampler and skimmer cones
616 of the mass spectrometer, ^{64}Zn is neglected in these studies. A clear odd-even staggering
617 was observed (Fig. 12).
618 Chromatographic experiments have also been run on crown ether resins (Ban et

al., 2002; Zhang et al., 2006; Fukuda et al., 2006). The isotope enrichment factors are mass-dependent within experimental errors, but odd-even staggering is permitted by the results (0.3-0.6‰ deviation from the mass-dependent line, Zhang et al., 2006).

6.8. Strontium

Strontium has four naturally occurring isotopes (^{84}Sr, ^{86}Sr, ^{87}Sr, and ^{88}Sr). Strontium isotope fractionation by chemical exchange reactions has been investigated by various research groups (Oi, et al., 1992; Nishizawa et al., 1994; 1995; Ban, et al., 2001; Shibahara et al., 2002b,c, 2003, 2006). On cation-exchange resins, the isotope separation factor per unit mass difference seems to be extremely small, ~1.000001 (Oi et al., 1992). Chromatographic systems in which macrocyclic compounds (crown ether and cryptand) are employed as the stationary phase improve the isotope separation factor by 100 times or more (Ban, et al., 2001; Shibahara et al., 2002b, 2003, 2006). Solvent extraction systems using a macrocyclic compound as an extractant also give large isotope separation factors (Nishizawa et al., 1994; 1995; Shibahara et al., 2002c).

Nishizawa et al. (1995) observed odd/even isotope staggering and a correlation between ε and $\langle r^2 \rangle$ (Fig. 13). The correlation is consistent with a nuclear field shift effect. A subsequent investigation (Shibahara et al., 2002c) supported it.

The mass-independent fractionation of Sr isotopes has also been examined by liquid chromatography with a cryptand stationary phase (Shibahara et al., 2002b, 2003, 2006). Isotopic abundances were analyzed by ICP-QMS, which makes the discussion of mass-independent isotope fractionation less certain. Ban et al. (2001) reported mass-dependent isotope fractionation of Sr by liquid chromatography with a crown ether as the stationary phase. A hint of mass-independent fractionation, however, can be

643 found in a sample (for example, sample D23).

644

645 *6.9. Zirconium*

646 Though mass-independent fractionations have been found in a liquid-liquid extraction
647 system (Fujii et al., 1998b), their profile did not show a simple dependence on $\langle r^2 \rangle$ (Fig.
648 5i).

649

650 *6.10. Molybdenum*

651 Molybdenum has seven naturally occurring isotopes, five even (^{92}Mo, ^{94}Mo, ^{96}Mo, ^{98}Mo,
652 and ^{100}Mo) and two odd (^{95}Mo and ^{97}Mo). Molybdenum isotopes were fractionated by
653 liquid-liquid extraction (Fujii et al, 2006c). The aqueous phase was Mo(VI) in HCl and
654 the organic phase was a dichloroethane solution containing a crown ether. Isotopic
655 analyses were performed by MC-ICP-MS with a precision of <100 ppm. Odd-even
656 staggering correlated with $\langle r^2 \rangle$ (Fig. 5j) was observed. Mass-independent isotope
657 fractionation was most conclusive in 5.4 M HCl (Fig. 14). The contributions of the
658 nuclear field shift effect and the mass effect were evaluated with Eq. 31. Figure 15a
659 shows the dependence of these contributions on HCl concentration. Mass-dependent
660 effects are predominant in concentrated acids, whereas the nuclear field shift effect was
661 most visible at HCl molalities < 6.5M.

662

663 *6.11. Ruthenium*

664 Ruthenium has seven naturally occurring isotopes, five even (^{96}Ru, ^{98}Ru, ^{100}Ru, ^{102}Ru,
665 and ^{104}Ru) and two odd (^{99}Ru and ^{101}Ru). Ruthenium isotopes were fractionated under
666 conditions similar to those described for Mo (Fujii et al., 2006c). Odd-even staggering

667 correlated with $<r^2>$ (Fig. 5k) can again be observed. ^{96}Ru and ^{98}Ru are neglected of the
668 discussion because of their small abundances. Mass-independent isotope fractionation
669 was found at high HCl molarity (Fig. 16). As with Mo, the relative contributions of the
670 nuclear field shift and mass effects (Fig. 15b) depend on HCl concentration.
671
672 *6.12. Tellurium*
673 Tellurium has eight naturally occurring isotopes, six even (^{120}Te, ^{122}Te, ^{124}Te, ^{126}Te, ^{128}Te,
674 and ^{130}Te) and two odd (^{123}Te and ^{125}Te). Tellurium isotopes were fractionated under the
675 same condition as Mo and Ru (Moynier et al, 2008). Odd-even staggering was observed
676 to correlate with $<r^2>$ (Fig. 5l). This suggests that fractionation of the odd atomic mass
677 isotope ^{125}Te deviates from the mass-dependent trend defined by the even atomic
678 isotopes (Fig. 17), and therefore should not be used for normalization (Fehr et al.,
679 2006).
680
681 *6.13. Barium*
682 Barium has seven naturally occurring isotopes, five even (^{130}Ba, ^{132}Ba, ^{134}Ba, ^{136}Ba, and
683 ^{138}Ba) and two odd (^{135}Ba and ^{137}Ba). ^{130}Ba and ^{132}Ba are less abundant isotopes. $<r^2>$
684 values of Ba isotopes show prominent odd-even staggering (Fig. 18a is reproduced from
685 Fig. 5m). There have been several studies of isotope fractionation of Ba in chemical
686 exchange reactions. These data (Nishizawa et al., 1994; Kondoh et al., 1996; Chang et
687 al., 1996; Shibahara et al., 2002a; Ban, 2002) are shown in Figs. 18b-f. In each system,
688 odd atomic mass isotopes are less fractionated than adjacent even atomic mass isotopes,
689 consistent with a nuclear field shift effect.
690

6.14. Lanthanides (cerium, neodymium, samarium, gadolinium, and ytterbium)

Cerium has no stable odd atomic mass isotopes (^{136}Ce, ^{138}Ce, ^{140}Ce, and ^{142}Ce). Thus odd-even staggering cannot be documented. ^{140}Ce possesses a magic number of neutron, 82. The variation of $<r^2>$ with isotopic mass is shown in Fig. 5n. Zhang et al. (2005) reported an unusual fractionation of Ce isotopes on a cation-exchange column (Fig. 19), but admitted uncertainty about possible Ba isobaric interferences at masses 136 and 138. Ce is a heavy element, the $<r^2>$ of the four isotopes varies and their nuclear spins are all zero. Hence, Ce is an ideal candidate to investigate the nuclear field shift effect. Achieving high precision for isotopic analysis is hampered by the small abundance of ^{136}Ce and ^{138}Ce, and the potential isobaric interferences of ^{136}Ba and ^{138}Ba (and ^{138}La).

A strong increase of isotope shifts (Brix and Kopfermann, 1958) and $<r^2>$ (Kuhn, 1969) has been pointed out starting around neutron number 90 (Figs. 5o-q). Isotope pairs with neutrons 88 and 90 include ^{148}Nd-^{150}Nd, ^{150}Sm-^{152}Sm, and ^{152}Gd-^{154}Gd. For example, it has long been known that the three even atomic mass isotopes ^{150}Sm, ^{152}Sm, and ^{154}Sm do not give equidistant lines in atomic spectra (Schüler, and Schmidt, 1934; Herzberg, 1944) and this gave rise to the suggestion that the nuclear shape needed to be taken into account to explain isotopic shifts (Brix and Kopfermann, 1949). Nuclear deformation around neutron number 90 is discussed in the literature (Stacy, 1966; Kurn, 1969; King, 1984). In a series of separation studies of Nd, Sm, and Gd isotopes using iquid-liquid extraction (Fujii et al., 1998c, 1999, 2000), isotope fractionation has been found to be strongly mass-independent for these isotope pairs (Fig. 20a and Fig. 21a). This effect was only tested for even atomic mass isotopes whose nuclear spins are zero, and hence, the finding strengthens confidence in the importance of the nuclear field shift effect.

715 The separation of Sm isotopes has also been investigated by equilibrating
716 amalgam with aqueous solutions (Dembiński et al., 1998, 2001). Fractionation patterns
717 are consistent with nuclear field shift effects. An odd-even staggering of Sm isotope
718 fractionation was also found in crown ether systems (Fig. 20a) (Fujii et al., 1998c). In
719 contrast, odd-even staggering cannot be identified in the amalgam experiments of
720 Dembiński et al. (2001) (Fig. 20b). However, ε's of even atomic mass isotopes (^{148}Sm,
721 ^{150}Sm, ^{152}Sm, and ^{154}Sm) do not follow a mass-dependent line (Fig 20b).
722 Odd-even staggering in Yb isotope fractionation was observed in the
723 experiments of Dembiński (1998, 2001). The odd-even staggering was also reported
724 previously by Chen et al. (1992) for ^{157}Gd and later by Ismail et al. (2000) for ^{155}Gd and
725 ^{157}Gd (Fig. 21b) who attributed the staggering to nuclear field shift effects.
726
727 *6.15. Hafnium*
728 The separation of Hf isotopes has been investigated in liquid-liquid extraction systems
729 with various extractants (Fujii et al., 2001b). No isotope fractionation was observed
730 among even isotopes (^{178}Hf and ^{180}Hf), but an effect was observed for the isotopes ^{177}Hf
731 and ^{179}Hf. It was suggested by the authors that the effect may result from the difference
732 of nuclear spins, I=7/2 for ^{177}Hf and 9/2 for ^{179}Hf.
733
734 *6.16. Actinides (Uranium)*
735 The history of the uranium isotope separation by chemical exchange has been reviewed
736 elsewhere (Bigeleisen, 1992, 2006; Ishida and Fujii, 2006). The nuclear field shift effect
737 was found in the unusual isotope enrichment of ^{235}U in a redox system (Fujii et al.,
738 1989a,b). Their results are shown in Fig. 22 (for comparison, $<r^2>$ profile is shown in

739 Fig. 5t). This finding prompted an update of the classic theory (Urey, 1947; Bigeleisen
740 and Mayer, 1947) by Bigeleisen (1996a) and Nomura et al. (1996). The relative
741 importance of quadrupole terms in the nuclear field shift of these isotopes was found by
742 Knyazev (1999, 2001) to be as large as 20 percent of the mean effect of nuclear size and
743 shape. The contribution of Bigleisen's (1996) theory to the uranium isotope separation
744 was reviewed by Mioduski (1999). In the most recent studies on *ab initio* molecular
745 orbital calculation (Abe at al., 2008a,b), the nuclear field shift effect found by Fujii et al.
746 (1989a,b) was reproduced.
747
748 In the latest studies, the nuclear field shift effects of Cd (Fujii et al., 2009) and Sn
749 (Moynier et al., 2009) have been found.
750
751 **7. Summary**
752 Over a decade has passed since Bigeleisen formulated his theory of the nuclear field
753 shift effect. With the advent of very precise mass spectrometers and the development of
754 computer simulations, experimental evidence of the ubiquity of the nuclear field shift is
755 increasing while at the same time the theoretical understanding of this process is
756 becoming stronger. The nuclear field shift effect is a suitable explanation of
757 mass-independent isotope fractionation in many equilibrium systems. By further
758 exploring the concepts laid out by Bigeleisen and their consequences, a better
759 understanding of mass-independent isotope fractionation should be achieved.
760
761 **Acknowledgment**
762 The authors thank Edwin Schauble, an anonymous reviewer, the guest editor, Mathieu

763 Roskosz, and the editor, Bernard Bourdon, for useful suggestions and constructive
764 comments on the manuscript. TF thanks Masabumi Miyabe for his valuable comments
765 to the nuclear spin effect and Roy Jacobus for his help in improving the English of the
766 manuscript.
767

References

Abe, M., Suzuki, T., Fujii, Y., Hada, M., 2008a. An *ab initio* study based on a finite nucleus model for isotope fractionation in the U(III)-U(IV) exchange reaction system. J. Chem. Phys. 128, 144309.

Abe, M., Suzuki, T., Fujii, Y., Hada, M., Hirao, K., 2008b. An *ab initio* molecular orbital study of the nuclear volume effects in uranium isotope fractionations. J. Chem. Phys. 129, 164309.

Angeli, I., 2004. A consistent set of nuclear rms charge radii: properties of the radius surface $R(N,Z)$. Atom. Data Nucl. Data Tables 87, 185-206.

Atkins, P. W., 1998. Physical Chemistry. 6th ed. Oxford University Press, Oxford.

Aufmuth, P., Heilig, K., Steudel, A., 1987. Changes in mean-square nuclear charge radii from optical isotope shifts. At. Data Nucl. Data Tables 37, 455-490.

Ban, Y., Nomura, M., Fujii, Y., 2001. Isotope effects of strontium in crown ether chromatography, Sep. Sci. Technol. 36, 2165-2180.

Ban, Y., 2002. Doctoral thesis, Tokyo Institute of Technology, Japan (in Japanese).

Ban, Y., Nomura, M., Fujii, Y., 2002. Isotope effects of zinc in crown ether chromatography. J. Nucl. Sci. Technol. 39, 156-159.

Bergquist, B. A., Blum, J. D., 2007. Mass-dependent and -independent fraction of Hg isotopes by photoreduction in aquatic systems. Science 318, 417-420.

Bigeleisen, J., Mayer, M. G., 1947. Calculation of equilibrium constants for isotopic exchange reactions. J. Chem. Phys. 15, 261-267.

Bigeleisen, J., 1992. History and theory of uranium isotope enrichment by chemical exchange. Bull. Res. Lab. Nucl. React. 16 (special issue 1), 3-17.

Bigeleisen, J., 1996a. Nuclear size and shape effects in chemical reactions. Isotope chemistry of the heavy elements. J. Am. Chem. Soc. 118, 3676-3680.

Bigeleisen, J., 1996b. Temperature dependence of the isotope chemistry of the heavy elements. Proc. Natl. Acad. Aci. USA 93, 9393-9396.

Bigeleisen, J., 1998. Second-order correction to the Bigeleisen-Mayer equation due to the nuclear field shift. Proc. Natl. Acad. Aci. USA 95, 4808-4809.

Bigeleisen, J., 2006. Theoretical basis of isotope effects from an autobiographical perspective. in Isotope Effects in Chemistry and Biology (Kohen, A., Limbach, H.-H., eds.), pp. 1-39, Taylor & Francis, Boca Raton.

Bizzarro, M., Ulfbeck, D., Trinquier, A., Thrane, K., Connelly, J. N., Meyer, B. S. 2007. Evidence for a late supernova injection of ^{60}Fe into the protoplanetary disk. Science 316, 1178-1181.

803 Breit, G., 1958. Theory of isotope shift. Rev. Mod. Phys. 30, 507-517.

804 Brix. P., Kopfermann, H., 1949. Zur isotopieverschiebung im spektrum des samariums.
805 Z. Phys. B 126, 344-364.

806 Brix. P., Kopfermann, H., 1958. Isotope shift studies of nuclei. Rev. Mod. Phys. 30,
807 517-520.

808 Buchachenko, A. L., 1977. Enrichment of magnetic isotopes - New method of
809 investigation of chemical reaction mechanisms. Russian J. Phys. Chem. 51,
810 1445-1451.

811 Buchachenko, A. L., 1995. MIE versus CIE: Comparative analysis of magnetic and
812 classical isotope effects. Chem. Rev. 95, 2507-2528.

813 Buchachenko, A. L., 2000. Recent advance in spin chemistry. Pure Appl. Chem. 72,
814 2243-2258.

815 Buchachenko, A. L., 2009. Magnetic isotope effects in chemistry and biochemistry.
816 Wiley Interscience, New York.

817 Chang, Z., Nomura, M., Motomiya, K., Fujii, Y., 1996. Isotope effects of barium in
818 amalgam/aqueous hydroxide solution systems. J. Chem. Soc., Faraday Trans. 92,
819 4485-4489.

820 Chen, J. R., Nomura, M., Fujii, Y., Kawakami, F., Okamoto, M., 1992. Gadolinium
821 isotope separation by cation exchange chromatography. J. Nucl. Sci. Technol. 29,
822 1086-1092.

823 Dauphas. N., Rouxel, O., 2006. Mass spectrometry and natural variations of iron
824 isotopes. Mass Spectrom. Rev. 25, 515-550.

825 Dauphas, N., Cook, D. L., Sacarabany, A., Fröhlich, C., Davis, A. M., Wadhwa, M.,
826 Pourmand, A., Rauscher, T., Gallino, R., 2008. Iron 60 evidence for early injection
827 and efficient mixing of stellar debris in the protosolar nebula. Astrophys. J. 686,
828 560-569.

829 Dembiński, W., Poniński, M., Fiedler, R., 1998. Preliminary results of the studies on
830 fractionation of ytterbium isotopes in Yb(III)-acetate/Yb-amalgam system. Sep. Sci.
831 Technol. 33, 1693-1701.

832 Dembiński, W., Poniński, M., Fiedler, R., 2001. Isotope effects of samarium and
833 ytterbium in the acetate/amalgam separation system. J. Radioanal. Nucl. Chem. 250,
834 423-428

835 Farquhar, J., Bao, H., Thiemens, M., 2000. Atmospheric influence of earth's earliest
836 sulfur cycle. Science 289, 756-758.

837 Fehr, M. A., Rehkamper, M., Halliday, A. N., Schonbachler, M., Hattendorf, B., Gunther,
838 D., 2006., Search for nucleosynthetic and radiogenic tellurium isotope anomalies in
839 carbonaceous chondrites. Geochim. Cosmochim. Acta 70, 3436-3448.

840 Fricke, G., Heilig, K., 2004. Nuclear Charge Radii (Landolt-Bornstein Numerical Data
841 and Functional Relationships in Science and Technology - New Series) (H. Schopper,
842 ed.), Springer, Berlin.

843 Fujii, T., Inagawa, J., Nishizawa, K., 1998a. Influences of nuclear mass, size, shape and
844 spin on chemical isotope effect of titanium. Ber. Bunsenges. Phys. Chem. 102,
845 1880-1885.

846 Fujii, T., Yamamoto, T., Inagawa, J., Watanabe, K., Nishizawa, K., 1998b. Influences of
847 nuclear size and shape and nuclear spin on chemical isotope effect of
848 zirconium-crown complex. Ber. Bunsenges. Phys. Chem. 102, 663-669.

849 Fujii, T., Yamamoto, T., Nishizawa, K., Inagawa, J., Gunji, K., Watanabe, K., , 1998c.
850 Separation of samarium isotopes by a crown ether. Sovent Ext. Ion Exch. 16,
851 985-999.

852 Fujii, T., Yamamoto, T., Inagawa, J., Gunji, K., Watanabe, K., Nishizawa, K., 1999.
853 Nuclear size and shape effect in chemical isotope effect of gadolinium using
854 dicyclohexano-18-crown-6. Sovent Ext. Ion Exch. 17, 1219-1229.

855 Fujii, T., Yamamoto, T., Inagawa, J., Gunji, K., Watanabe, K., Nishizawa, K., 2000.
856 Nuclear size and shape effect in chemical isotope enrichment of neodymium using
857 dicyclohexano-18-crown-6. Sovent Ext. Ion Exch. 18, 1155-1166.

858 Fujii, T., Hirata, T., Shibahara, Y., Nishizawa, K., 2001a. Mass-dependent and
859 mass-independent isotope effects of zinc in chemical exchange reactions using liquid
860 chromatography with a cryptand stationary phase. Phys. Chem. Chem. Phys. 3,
861 3125-3129.

862 Fujii, T., Moriyama H., Hirata, T., Nishizawa, K., 2001b. Isotope effects of hafnium in
863 solvent extraction using crown ethers. Bull. Chem. Soc. Jpn. 74, 1031-1032.

864 Fujii, T., Suzuki, D., Gunji, K., Watanabe, K., Moriyama, H., Nishizawa, K., 2002.
865 Nuclear field shift effect in the isotope exchange reaction of chromium(III) using a
866 crown ether. J. Phys. Chem. A 106, 6911-6914.

867 Fujii, T., Suzuki, D., Watanabe, K., Yamana, H., 2006a. Application of the total
868 evaporation technique to chromium isotope ratio measurement by thermal ionization
869 mass spectrometry. Talanta 69, 32-36.

870 Fujii, T., Moynier. F, Telouk, P., Albarède, F. 2006b. Isotope fractionation of iron(III) in
871 chemical exchange reactions using solvent extraction with crown ether. J. Phys.
872 Chem. A 110, 11108-11112.

873 Fujii, T., Moynier. F, Telouk, P., Albarède, F. 2006c. Mass-independent isotope
874 fractionation of molybdenum and ruthenium and the origin of isotopic anomalies in
875 Murchison. Astrophys. J. 647, 1506-1516.

876 Fujii, T., Moynier, F., Yin, Q-Z., 2007. Mass-independent isotope fractionation of
877 chromium in ligand exchange reaction and redox reaction. Lunar Planet. Sci. Conf.
878 38, 1213.

879 Fujii, T., Moynier, F., Yin, Q-Z., Yamana, H., 2008a. Mass-independent isotope
880 fractionation in the chemical exchange reaction of chromium(III) using a crown ether.
881 J. Nucl. Sci. Technol. suppl. 6, 6-9.

882 Fujii, T., Suzuki, D., Yamana, H., 2008b. Nuclear field shift effect of chromium(III) in
883 repeated extraction using a crown ether. Solvent Extr. Ion Exch. 26, 100-112.

884 Fujii, T., Moynier. F, Telouk, P., Albarède, F., 2009. Nuclear field shift effect in the
885 isotope exchange reaction of cadmium using a crown ether. Chem. Geol.
886 doi:10.1016/j.chemgeo.2008.12.004.

887 Fujii, Y., Hoshi, J., Iwamoto, H., Okamoto, M., Kakihana, H., 1985. Calcium isotope
888 effects in ion exchange electromigration and calcium isotope analysis by
889 thermo-ionization mass spectrometry. Z. Naturforsch. 40a, 843-848.

890 Fujii, Y., Nomura, M., Okamoto, M., Onitsuka, H., Kawakami, F., Takeda, K., 1989a.
891 An anomalous isotope effect of ^{235}U in U(IV)-U(VI) chemical exchange. Z.
892 Naturforsch. A 44, 395-398.

893 Fujii, Y., Nomura, M., Onitsuka, H., Takeda, K., 1989b. Anomalous isotope frctionation
894 in uranium enrichment process. J. Nucl. Sci. Technol. 26, 1061-1064.

895 Fukuda, Y., Zhang, Y. -H., Suzuki, T., Fujii, Y., Oi, T., 2006. Zinc isotope accumulation
896 in liquid chromatography with crown ether resin. J. Nucl. Sci. Technol. 43, 446-449.

897 Glueckauf, E., 1955. Theory of chromatography. Part 9. The "theoretical plate" concept
898 in column separations. Trans. Faraday Soc. 51, 34-44.

899 Hathorn, B. C. Marcus, B. C., 1999. An intramolecular theory of the mass-independent
900 isotope effect for ozone. I. J. Chem. Phys. 111, 4087-4100.

901 Heilig, K., Steudel, A., 1978. *in* Progress in Atomic Spectroscopy (W. Hanle and H.
902 Kleinpoppen, eds.), Part A, pp. 263-328, Plenum Press, New York.

903 Herzberg, G., 1944. Atomic spectra and atomic structure. Dover Publications, New
904 York.

905 Heumann, K. G., Schiefer, H. -P., 1980. Calcium isotope separation on an exchange
906 resin having cryptand anchor groups. Angew. Chem. Int. Ed. Engl. 19, 406-407.

907 Heumann, K. G., Schiefer, H. -P., Spiess, W., 1982. Enrichment of heavy calcium
908 isotopes by ion exchange resins with cyclopolyethers as anchor groups. in Stable
909 Isotopes (Schiefer, H. -P., Förstel, H., Heinzinger, K., eds.), pp. 711-718, Elsevier,
910 Amsterdam.

911 Heumann, K. G., 1985. Isotopic separation in systems with crown ethers and cryptands.
912 *in* Topics in Current Chemistry (K. Meurer, ed.), vol. 127, pp. 77-132, Springer,
913 Berlag.

914 Hutchison, C. A., Stewart, D. W., Urey, H. C., 1940. The concentration of C^{13}. J. Chem.
915 Phys. 8, 532-537.

916 Ishida, T. 2002. Isotope effect and isotope separation: A chemist's view. J. Nucl. Sci.
917 Technol. 39, 407-412.

918 Ishida, T., Fujii Y., 2006. Enrichment of isotopes. in Isotope Effects in Chemistry and
919 Biology (Kohen, A., Limbach, H.-H., eds.), pp. 41-87, Taylor & Francis, Boca
920 Raton.

921 Ismail, I. M., Fukami, A., Nomura, M., Fujii, Y., 2000. Anomaly of ^{155}Gd and ^{157}Gd
922 isotope effects in ligand exchange reactions observed by ion exchange
923 chromatography. Anal. Chem. 72, 2841-2845.

924 Jepson, B. E., Shockey, G. C., 1984. Calcium hydroxide isotope effect in calcium
925 isotope enrichment by ion exchange. Sep. Sci. Technol., 19, 173-181.

926 Jepson, B. E., Cairns, G. A., 1979. Lithium isotope effects in chemical exchange with
927 (2,2,1) cryptand. MLM-2622.

928 Kakihana H., Kanzaki T., 1969. A simplified and generalized method for analyzing
929 chromatographic isotope separation fata. Bull. Tokyo Inst. Technol., 90, 77-89.

930 Kawashiro. F., Fujii, T., Nishizawa, K., 1998. Mass-independent isotope effects in
931 chemical exchange reaction. Chromium isotope enrichment by a crown ether. in Proc.
932 Sep. Phenomena Liq. Gases (Yamamoto, I., ed), pp.391-399, Nagoya Univ.

933 Khudyakov, I. V., Serebrennikov, Y. A., Turro, N. J., 1993. Spin-orbit coupling free
934 radical reactions: On the way to heavy elements. 93, 537-570.

935 King, W. H., 1984. Isotope shifts in atomic spectra. Plenum Press, New York.

936 Kleinman L. I., Wolfsberg. M., 1973. Corrections to Born-Oppenheimer approximation
937 and electronic effects on isotopic-exchange equilibria. J. Chem. Phys. 59, 2043-2053.

938 Kleinman L. I., Wolfsberg. M., 1974a. Corrections to Born-Oppenheimer approximation
939 and electronic effects on isotopic-exchange equilibria. II. J. Chem. Phys. 60,
940 4740-4748.

941 Kleinman L. I., Wolfsberg. M., 1974b. Shifts in vibrational constants from corrections
942 to Born-Oppenheimer approximation: Effects on isotopic-exchange equilibria. J.
943 Chem. Phys. 60, 4749-4754.

944 Knyazev, D. A., Semin, G. K., Bochkarev, A. V., 1999. Nuclear quadrupole contribution
945 to the equilibrium isotope effect. Polyhedron 18, 2579-2582.

946 Knyazev, D. A., Myasoedov, N. F., 2001. Specific effects of heavy nuclei in chemical
947 equilibrium. Sep. Sci. Technol., 36, 1677-1696.

948 Kondoh, A., Oi, T., Hosoe, M., 1996. Fractionation of barium isotopes in
949 cation-exchange chromatography. Sep. Sci. Technol. 31, 39-48.

950 Kotaka, M., Okamoto, M., Bigeleisen, J., 1992. Anomalous mass effects in isotopic
951 exchange equilibria. J. Am. Chem. Soc. 114, 6436-6445.

952 Kurn, H. G., 1969. Atomic spectra. Longman's, London.

953 Lawler, R. G., Evans, G. T., 1971, Some chemical consequences of magnetic interactions
954 in radical pairs. Ind. Chim. Belg. 36, 1087-1089.

955 London, H. 1961. Separation of isotopes. George Newnes Limited, London.

956 Mioduski, T., 1999. Comment to the Bigeleisen's theory of isotope chemistry of the
957 heavy elements. Comments Inorg. Chem. 21, 175-196.

958 Minkin, V. I., 1999. Glossary of terms used in theoretical organic chemistry. Pure Appl.
959 Chem. 10, 1919-1981.

960 Moynier, F., Yin, Q-Z., Jacobsen, B., 2007a. Dating the first stage of planet formation.
961 Astrophys. J. Lett. 671, L181-L183.

962 Moynier, F., Blichert-Toft, J., Telouk, P., Luck J.-M., Albarède, F., 2007b. Comparative
963 stable isotope geochemistry of Ni, Cu, Zn, and Fe in chondrites and iron meteorites.
964 Geochim. Cosmochim. Acta 71, 4365-4379.

965 Moynier, F., Fujii, T., Telouk, P., Albarède, F., 2008. Isotope separation of Te in
966 chemical exchange system with dicyclohexano-18-crown-6. J. Nucl. Sci. Technol.
967 suppl. 6, 10-14.

968 Moynier, F., Fujii, T., Telouk, P., 2009. Mass-independent isotopic fractionation of tin in
969 chemical exchange reaction using a crown ether. Anal. Chim. Acta. 632, 234-239.

970 Nishizawa, K., Ishino. S., Watanabe, H., Shinagawa, M., 1984. Lithium isotope
971 separation by liquid-liquid extraction using benzo-15-crown-5. J. Nucl. Sci. Technol.
972 21, 694-701.

973 Nishizawa, K., Nakamura, K., Yamamoto, T., Masuda, T., 1993. Zinc isotope effects in
974 complex-formation with a crown-ether. Solvent Extr. Ion Exch. 11, 389-394.

975 Nishizawa, K., Nakamura, K., Yamamoto, T., Masuda, T., 1994. Separation of strontium
976 and barium isotopes using a crown-ether. Different behaviors of odd mass and even
977 mass isotopes. Solvent Extr. Ion Exch. 12, 1073-1084.

978 Nishizawa, K., Satoyama, T., Miki, T., Yamamoto, T., Hosoe, M., 1995. Strontium
979 isotope effect in liquid-liquid extraction of strontium chloride using a crown ether. J.
980 Nucl. Sci. Technol. 32, 1230-1235.

981 Nishizawa, K., Satoyama, T., Miki, T., Yamamoto, T., Nomura, M., 1996. Separation of
982 zinc isotopes by liquid-liquid extraction using a crown ether. Sep. Sci. Technol. 31,
983 2831-2841.

984 Nishizawa, K., Miki, T., Ikeda, R., Fujii, T., Yamamoto, T., Nomura, M., 1997. Isotopic
985 enrichment of nickel in aqueous solution/crown ether system. J. Mass Spectrom. Soc.
986 Jpn. 45, 521-527.

987 Nishizawa, K., Miki, T., Satoyama, T., Fujii, T., Yamamoto, T., Nomura, M., 1998a.
988 Enrichment of zinc isotopes by a liquid membrane system using a crown ether. Sep.
989 Sci. Technol. 33, 991-1002.

990 Nishizawa, K., Maeda, Y., Kawashiro, F., Fujii, T., Yamamoto, T., Hirata, T., 1998b.
991 Contributions of nuclear size and shape, nuclear mass, and nuclear spin to
992 enrichment factors of zinc isotopes in a chemical exchange reaction by a cryptand.
993 Sep. Sci. Technol. 33, 2101-2112.

994 Nomura, M., Higuchi, N., Fujii, Y., 1996. Mass dependence of uranium isotope effects
995 in the U(IV)-U(VI) exchange reaction. J. Am. Chem. Soc. 118, 9127-9130.

996 Oi, T., Ogino, H., Hosoe, M., Kakihana, H., 1992. Fractionation of strontium isotopes in
997 cation-exchange chromatography. Sep. Sci. Technol. 27, 631-643.

998 Oi, T., Morioka, N., Ogino, H., Kakihana, H., Hosoe, M., 1993. Fractionation of
999 calcium isotopes in cation-exchange chromatography. Sep. Sci. Technol. 28,
1000 1971-1983.

1001 Quitté, G., Halliday, A. N., Meyer, B. S., Markowski, A., Latkoczy, C., Günther, D.,
1002 2007. Correlated iron 60, nickel 62, and zirconium 96 in refractory inclusions and the
1003 origin of the solar system. Astrophys. J. 655, 678-684.

1004 Rai, V. K., Thiemens M. H., 2007. Mass independently fractionated sulfur components
1005 in chondrites. Geochim. Cosmochim. Acta 71, 1341–1354.

1006 Regelous, M., Elliott, T., Coath, C. D., 2008. Nickel isotope heterogeneity in the early
1007 Solar System. Earth Planet. Sci. Lett. 272, 330-338.

1008 Rykov, S. V., Khudyakov, I. V., Skakovsky, E. D., Tychinskaya, L. Yu., Ogorodnikova,
1009 M. M. 1992. Magnetic and spin effects furing dioxouranium(VI) sussinate photolysis.
1010 J. Photochem. Photobiol. A 66, 127-130.

1011 Salikhov, K. M., 1996. Magnetic isotope in radical reactions. Springer, Verlag/Wien.

1012 Schauble, E. A., 2007. Role of nuclear volume in driving equilibrium stable isotope
1013 fractionation of mercury, thallium, and other very heavy elements, Geochim.
1014 Cosmochim. Acta 71, 2170-2189.

1015 Schlembach, J., Tiemann, E., 1982. Isotope field shift of the rotational energy of the
1016 Pb-chalcogenides and Tl-halides. Chem. Phys. 68, 21-28.

1017 Schüler, H., Schmidt, Th., 1934. Über eine neue erscheinung bei den isotopen des
1018 samariums. Z. Phys. 92, 148-152.

1019 Shibahara, Y., Nomura, M., Hamanishi, E., Suzuki, K., Fujii, T., 2002a. Temperature
1020 dependence of isotope effects of barium using a crown ether, (II). Barium isotope
1021 effects in $BaCl_2$/DC18C6 systems. J. Nucl. Sci. Technol. 39, 938-940.

1022 Shibahara, Y., Nishizawa, K., Yasaka, Y., Fujii, T., 2002b. Strontium isotope effect in
1023 DMSO-water system by liquid chromatography using a cryptand polymer. Solvent
1024 Extr. Ion Exch., 20, 67-79.

1025 Shibahara, Y., Takaishi, H., Nishizawa, K., Fujii, T., 2002c. Strontium isotope effects in
1026 ligand exchange reaction. J. Nucl. Sci. Technol. 39, 451-456.

1027 Shibahara, Y., Nishizawa, K., Yasaka, Y., Fujii, T., 2003. Effect of counter anion in
1028 isotope exchange reaction of strontium, Solvent Extr. Ion Exch., 21, 435-448.

1029 Shibahara, Y., Yasaka, Y., Izumi, Y., Ema, K., Takeda, S., Nishijima, S., Fujii, T., 2006.
1030 Solvent effect in isotope exchange reaction of strontium by liquid chromatography
1031 using a cryptand (2_B,2,2) polymer, Solvent Extr. Ion Exch., 24, 915-929.

1032 Spedding, F. H., Powell, J. E., Svec, H. J., 1955. A laboratory method for separating
1033 nitrogen isotopes by ion exchange. J. Am. Chem. Soc. 77, 6125-6132.

1034 Stacey, D. N., 1966. Isotope shifts and nuclear charge distributions, Rep. Prog. Phys. 29,
1035 171-215.

1036 Step, E. N., Buchachenko, A. L., Turro, N. J., 1992. Magnetic effects in the photolysis
1037 of micellar solutions of phenacylphenylsulfone. Chem. Phys. 162, 189-204.

1038 Stern R. C., Snavely B. B., 1976. The laser isotope separation program at lawrence
1039 livermore laboratory. Ann. NY Acad. Sci. 267, 71-80.

1040 Stewart, D. W., Cohen, K., 1940. The further concentration of S^{34}. J. Chem. Phys. 8,
1041 904-907.

1042 Tiemann, E., Knöckel, H., Schlembach, J., 1982. Influence of the finite size on the
1043 electronic and rotational energy of diatomic molecules. Ber. Bunsenges. Phys. Chem.
1044 86, 821-824.

1045 Thiemens, M. H., 2006. History and application of mass-independent isotope effects.
1046 Annu. Rev. Earth Planet Sci. 34, 217-262.

1047 Turro, N. J., 1983. Influence of nuclear spin on chemical reactions: Magnetic isotope
1048 and magnetic field effects (A review). Proc. Natl. Acad. Sci. USA 80, 609-621.

1049 Urey, H. C., Huffman, J. R., Thode, H. G., Fox, M., 1937. Concentration of N^{15} by
1050 chemical methods. J. Chem. Phys. 5, 856-868.

1051 Urey, H. C., 1947. The thermodynamic properties of isotopic substances. J. Chem. Soc.
1052 562-581.

1053 Wakasa, M., Hayashi H., Kobayashi T., Takada, T., 1993. Enrichment of germanium-73
1054 with the magnetic isotope effect. J. Phys. Chem. 97, 13444-13446.

1055 Wakasa M., Hayashi H., Ohara, K., Takada, T., 1998. Enrichment of germanium-73 with
1056 the magnetic isotope effect on the hydrogen abstraction reaction of triplet
1057 benzophenone with triethylgermane in an SDS miceller solution. J. Am. Chem. Soc.
1058 120, 3227-3230.

1059 Watanabe, Y., Ohmoto, H., 2007. Mass independent fractionation of sulfur isotopes
1060 during thermochemical sulfate reduction: Implications to the biosphere evolution.
1061 Astrobiology 7, 533-533.

1062 Watanabe, Y., Farquhar, J., Ohmoto, H., 2009. Anomalous fractionations of sulfur
1063 isotopes during thermochemical sulfate reduction. Science 324, 370-373.

1064 Weston, Jr., R. E., 1999, Anomalous or mass-independent isotope effects. Chem. Rev.
1065 99, 2115-2136.

1066 Yin, Q-Z., Jacobsen, B., Moynier, F., Hutcheon, I. D., 2007. Toward consistent
1067 chronology in the early solar system: High-resolution ^{53}Mn-^{53}Cr chronometry for
1068 chondrules. Astrophys. J. 662, L43-L46.

1069 Zhang, Y. -H., Gunji, S., Nomura, M., Fujii, Y., Oi, T., 2005. Observation of cerium
1070 isotope fractionation in ion-exchange chromatography of Ce(III)-malate complex.

1071 Zhang, Y. -H., Fukuda, Y., Nomura, M., Fujii, Y., Oi, T., 2006. Zinc isotope effects
1072 observed by liquid chromatography with benzo-15-crown-5-resin. J. Nucl. Sci.
1073 Technol. 43, 415-418.
1074

1075
1076

1077 Table 1 Mass-independent isotope fractionations found in laboratory-scale chemical exchange
1078 experiments which suggest the nuclear field shift effect.

	Reaction	Method	Isotopic analysis	Reference
Ca	Ligand exchange	Liquid chromatography	TIMS	Heumann et al., 1982
	Ligand exchange	Liquid membrane	TIMS	Fujii et al., 1985
	Ligand exchange	Liquid chromatography	TIMS	Oi et al., 1993
Ti	Ligand exchange	Solvent extraction	MC-TIMS	Fujii et al., 1998a
Cr	Ligand exchange	Solvent extraction	TIMS	Kawashiro et al., 1998
	Ligand exchange	Solvent extraction	MC-TIMS	Fujii et al., 2002
	Ligand exchange	Solvent extraction	MC-ICP-MS	Fujii et al., 2007
	Redox	Pyrometallurgical extraction	MC-ICP-MS	Fujii et al., 2007
	Ligand exchange	Solvent extraction	MC-ICP-MS	Fujii et al., 2008a
	Ligand exchange	Repeated extraction	MC-TIMS	Fujii et al., 2008b
Ni	Ligand exchange	Solvent extraction	TIMS	Nishizawa et al., 1997
Zn	Ligand exchange	Solvent extraction	ICP-QMS	Nishizawa et al., 1993
	Ligand exchange	Solvent extraction	TIMS	Nishizawa et al., 1996
	Ligand exchange	Liquid membrane	TIMS	Nishizawa et al., 1998a
	Ligand exchange	Liquid chromatography	MC-ICP-MS	Nishizawa et al., 1998b
	Ligand exchange	Liquid chromatography	MC-ICP-MS	Fujii et al., 2001a
	Ligand exchange	Liquid chromatography	ICP-QMS	Zhang et al., 2006
Sr	Ligand exchange	Solvent extraction	TIMS	Nishizawa et al., 1994
	Ligand exchange	Solvent extraction	TIMS	Nishizawa et al., 1995
	Ligand exchange	Liquid chromatography	TIMS	Ban et al., 2001
	Ligand exchange	Liquid chromatography	ICP-QMS	Shibahara et al., 2002b
	Ligand exchange	Solvent extraction	TIMS	Shibahara et al., 2002c
	Ligand exchange	Liquid chromatography	ICP-QMS	Shibahara et al., 2003
	Ligand exchange	Liquid chromatography	ICP-QMS	Shibahara et al., 2006
Mo	Ligand exchange	Solvent extraction	MC-ICP-MS	Fujii et al., 2006c
Ru	Ligand exchange	Solvent extraction	MC-ICP-MS	Fujii et al., 2006c
Te	Ligand exchange	Solvent extraction	MC-ICP-MS	Moynier et al., 2008
Ba	Ligand exchange	Solvent extraction	TIMS	Nishizawa et al., 1994
	Ligand exchange	Liquid chromatography	TIMS	Kondoh et al., 1996
	Redox	Electrolytic reduction	TIMS	Chang et al, 1996
	Ligand exchange	Solvent extraction	TIMS	Shibahara et al., 2002a
	Ligand exchange	Liquid chromatography	TIMS	Ban., 2002
Nd	Ligand exchange	Solvent extraction	MC-TIMS	Fujii et al., 2000

Sm	Ligand exchange	Solvent extraction	MC-TIMS	Fujii et al., 1998c
	Redox	Electrolytic reduction	MC-TIMS	Dembiński et al, 2001
Gd	Ligand exchange	Liquid chromatography	TIMS	Chen et al., 1992
	Ligand exchange	Solvent extraction	MC-TIMS	Fujii et al., 1999
	Ligand exchange	Liquid chromatography	TIMS	Ismail et al., 2000
Yb	Redox	Reduction extraction	MC-TIMS	Dembiński et al, 1998
	Redox	Reduction extraction	MC-TIMS	Dembiński et al, 2001
U	Redox	Liquid chromatography	TIMS	Fujii et al., 1989a,b

1079 TIMS: Thermal ionization mass spectrometry
1080 ICP-QMS: Inductively coupled plasma quadrupole mass spectrometry
1081 MC-TIMS: Multicollector thermal ionization mass spectrometry
1082 MC-ICP-MS: Multicollector inductively coupled plasma mass spectrometry
1083

Figure captions

Figure 1 Vibrational potential curves of isotopologues.

Figure 2 Electrostatic potentials of nuclei. (a) The Coulomb potential for a point nucleus. (b) The electrostatic potential for a nucleus of the same charge with a finite size of charge distribution. (c) The electrostatic potential for another nucleus with the same charge but a larger size of charge distribution.

Figure 3 Hyperfine splitting levels of a ^{235}U(III) complex. The ground state energy is set to be zero (see Table 2 in (Bigeleisen, 1996a)).

Figure 4 Applicability of the Bigleiesen's (1996) theory to experimental results at a constant temperature. The nuclear spin of the even isotopes is set to be zero, while odd isotopes have non-zero spin.

Figure 5 Changes in mean-square nuclear charge radii. Data and errors are from (Aufmuth, 1987) unless otherwise indicated. Isotopic differences are relative to the most abundant isotope. a) S (Angeli, 2004), b) Ca, c) Ti (Fricke and Heilig, 2004), d) Cr, e) Fe, f) Ni. g) Zn (only relative values of $\delta\langle r^2\rangle$ are available (Aufmuth, 1987)), h) Sr, i) Zr, j) Mo, k) Ru, l) Te (Fricke and Heilig, 2004), m) Ba, n) Ce, o) Nd, p) Sm, q) Gd, r) Yb, s) Hf, t) U.

Figure 6 Temperature dependence of isotope fractionation predicted by Bigleiesen's (1996) theory at various temperatures.

Figure 7 Vibrational potential curves of isotopologues (including transition state) in a chemical reaction.

Figure 8 Isotope enrichment factors of Ca. (a) Isotope fractionation of Ca at a distance x compared to that in original solution (cation exchange membrane system, 298 K (Fujii et al., 1985)). (b) Isotope fractionation of Ca between eluent and resin (cation exchange chromatography, 298K (acetate) (Oi et al., 1993)).

Figure 9 Isotope enrichment factors of Ti. Ti isotopes were fractionated by using a solvent extraction technique with a crown ether, (organic solution)/(HCl solution) (Fujii et al., 1998a). Errors are 2σ analytical errors. a) Ti(III), b) Ti(IV).

Figure 10 Isotope enrichment factors of Cr. Cr isotopes were fractionated by using a solvent extraction technique with a crown ether, (organic solution)/(HCl solution). Mass-dependent lines (dotted lines) were drawn for an isotope pair, ^{50}Cr-^{52}Cr. Errors are

2σ analytical errors. a) isotope fractionation of Cr in organic phase compared to that in an original solution (Fujii et al., 2007). The isotope enrichment factor for ^{54}Cr was an estimated value (Fujii et al., 2007, 2008a). b) isotope fractionation of Cr in aqueous phase compared to that in an original solution (Fujii et al., 2008b).

Figure 11 Isotope enrichment factors of Fe. Fe isotopes were fractionated by using a solvent extraction technique with a crown ether, (organic solution)/(HCl solution). In the extraction reaction, only a very small deviation from the mass-dependent property was observed. The reported ε(L) data (Fujii et al, 2006b) are plotted showing 2σ analytical errors. A mass-dependent line (dotted line) is shown for the isotope pair, ^{54}Fe-^{56}Fe. The isotope enrichment factor for ^{58}Fe was estimated by using Eq. 31.

Figure 12 Isotope enrichment factors of Zn. Zn isotopes were fractionated by liquid chromatography (Nishizawa et al., 1998b). A cryptand polymer was used as the stationary phase, and the liquid phase was a mixture of water-acetone-hydrochloric acid. Isotope fractionation of Zn between eluent (sample number 12) and resin was shown. The error bars are smaller than the data symbols.

Figure 13 Isotope enrichment factors and changes in mean-square radius in Sr. Open marks showed the result of Nishizawa et al. (1995) (isotope fractionation of Sr between organic phase and aqueous phase). The analytical errors of isotope ratio are reported to be less than 0.1% (1σ). The $\delta\langle r^2\rangle$ values and their errors are reproduced from (Aufmuth et al., 1987).

Figure 14 Isotope enrichment factors of Mo. Mo isotopes were fractionated using a solvent extraction technique with a crown ether, (organic solution)/(HCl solution). Enrichment factors obtained at 5.4 M HCl (Fujii et al. 2006c) are shown. 2σ analytical errors are also shown (detailed error evaluation method can be seen in (Fujii et al. 2006c)).

Figure 15 Dependence of nuclear field shift effect and mass-dependent fractionation of Mo and Ru. Relative contributions of nuclear field shift effect and mass-dependent fractionation to isotope enrichment factors of the isotope pairs ^{100}Mo-^{95}Mo and ^{104}Ru-^{99}Ru were evaluated with Eq. 31 in this article.

Figure 16 Isotope enrichment factors for Ru. Ru isotopes were fractionated using a solvent extraction technique with a crown ether, (organic solution)/(HCl solution). Enrichment factors obtained at 8.2 M HCl (Fujii et al. 2006c) are shown. The error bars are smaller than the data symbols. (details of the error evaluation method are in (Fujii et

al. 2006c)).

Figure 17 Isotope enrichment factors for Te. Te isotopes were fractionated using a solvent extraction technique with a crown ether, (organic solution)/(HCl solution). The enrichment factors obtained at 5.62 M HCl (Moynier et al. 2008) are shown. Errors are 2σ analytical errors. ^{120}Te and ^{123}Te are not shown.

Figure 18 Changes in mean-square charge radius and reported isotope enrichment factors for Ba. (a) $\delta\langle r^2\rangle$: Reproduced from Fig. 5(m). (b) ε values found in liquid-liquid extraction (Nishizawa et al., 1994). 2σ errors are shown. (c) ε values found in cation exchange chromatography with barium acetate (Kondoh et al., 1996). Analytical errors are not shown. (d) ε values found in an amalgam/aqueous solution system (Chang et al., 1996). Errors are 2σ. (e) ε values found in a liquid-liquid extraction system (Shibahara et al., 2002a). Errors are 2σ. (f) ε values found in ligand exchange chromatography with a crown ether (Run B-1) (Ban, 2002). Errors are 2σ.

Figure 19 Isotope enrichment factors for Ce in liquid chromatography. Isotope fractionation was measured between Ce(III)-malate and Ce ions on a cation-exchange resin (Zhang et al., 2005).

Figure 20 Isotope enrichment factors for Sm. a) Sm isotopes were fractionated using solvent extraction with a crown ether, (organic solution)/(HCl solution). Enrichment factors at 1 M HCl (Fujii et al., 1998c) are shown. Errors are 2σ. ^{144}Sm was not used for discussion. b) Isotope fractionation of Sm in a (Sm(III) acetate/Sm in amalgam) was studied (Dembiński et al., 2001). 2σ analytical errors are shown.

Figure 21 Isotope enrichment factors for Gd. a) Gd isotopes were fractionated using solvent extraction with a crown ether, (organic solution)/(HCl solution). Enrichment factors obtained at 2 M HCl (Fujii et al., 1999) are shown. Errors are 2σ. ^{155}Gd and ^{157}Gd were not used for discussion. b) Gd isotopes were fractionated in liquid chromatography. Isotope fractionation was measured between Gd(III)-EDTA and Gd ions on a cation-exchange resin (Ismail et al., 2000). Errors are 2σ.

Figure 22 Isotope enrichment factors for U. U isotopes were fractionated in liquid chromatography. Isotope fractionation in an U(IV)-U(VI) reaction was studied ((Fujii et al., 1989a,b)). The error bars are smaller than the data symbols. Isotope enrichment factors are referred in (Bigeleisen, 1996a).

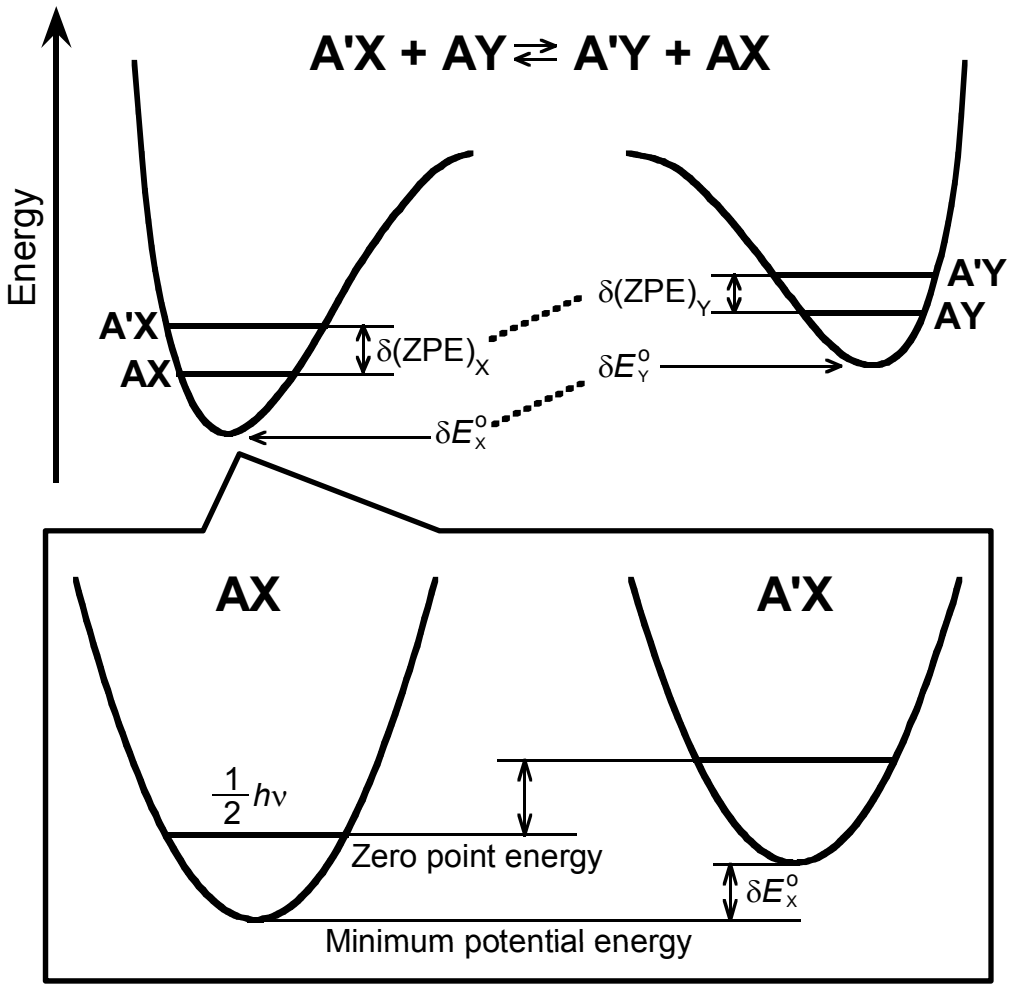
A'X + AY ⇄ A'Y + AX
Energy
A'X
AX
δ(ZPE)X
δ(ZPE)Y
A'Y
AY
δE°Y
δE°X
AX
A'X
½ hν
Zero point energy
δE°X
Minimum potential energy

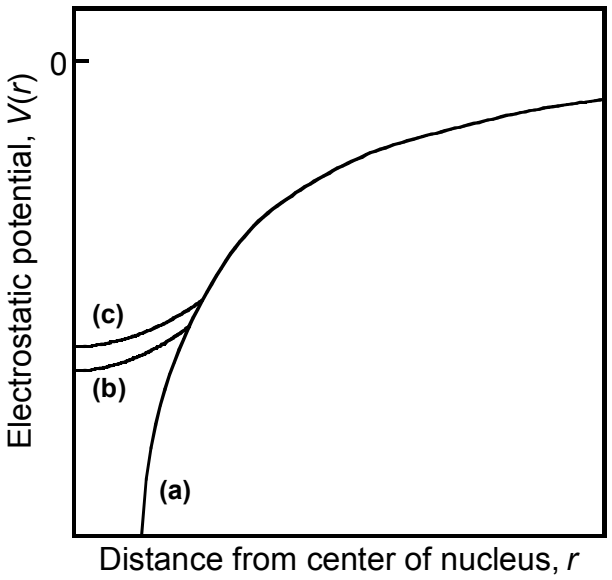
0
Electrostatic potential, V(r)
(c)
(b)
(a)
Distance from center of nucleus, r

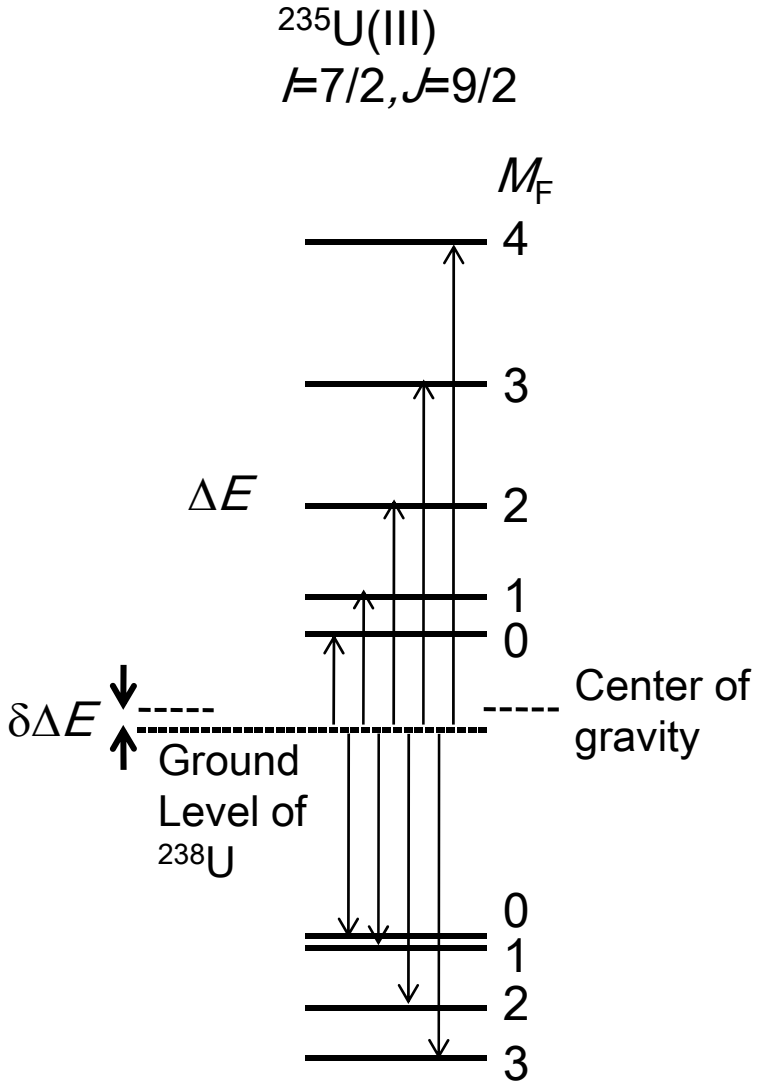
^{235}U(III)
I=7/2, J=9/2
M_F
4
3
ΔE
2
1
0
$\delta\Delta E$
Center of gravity
Ground Level of ^{238}U
0
1
2
3

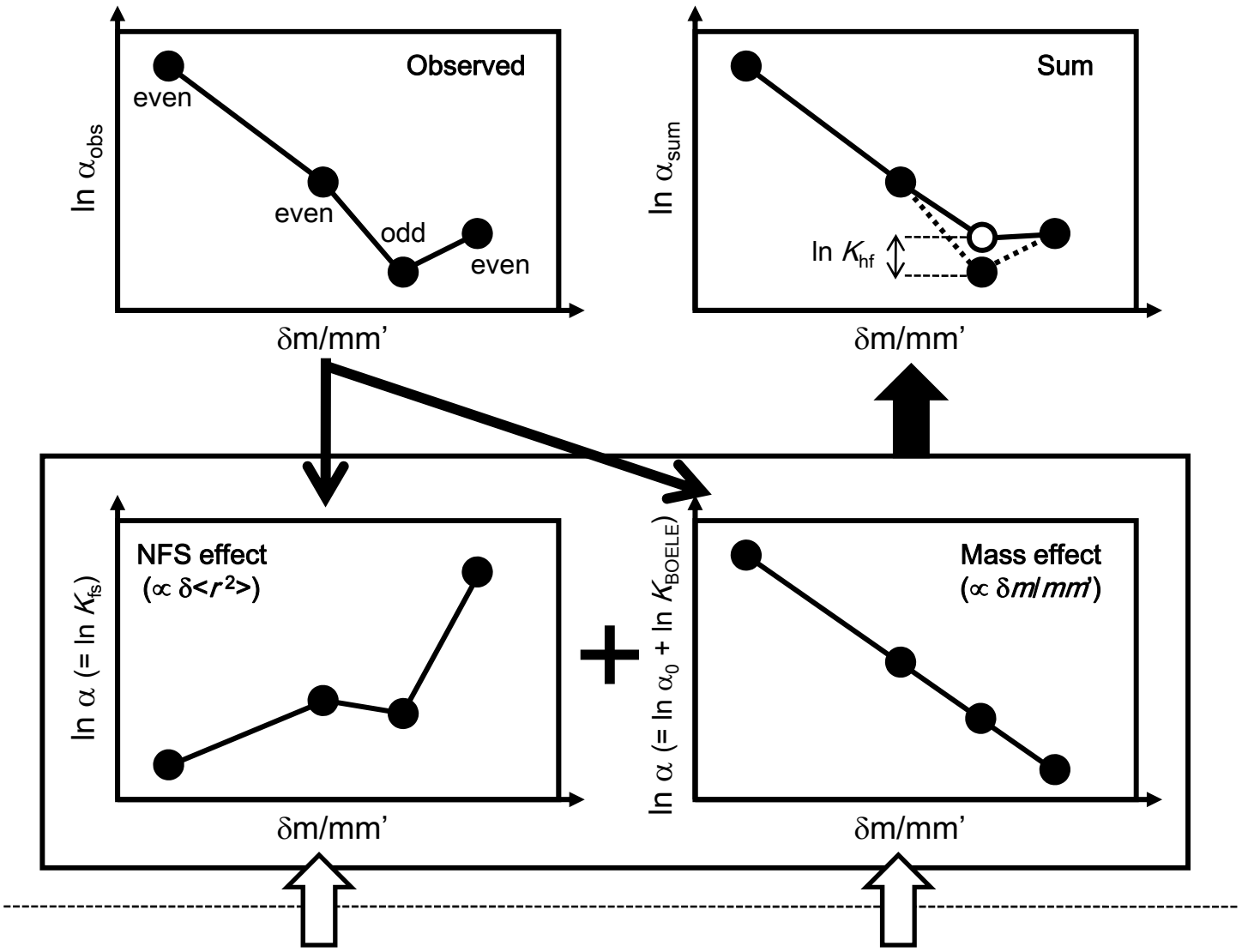

Theoretical
$\delta E°$ evaluation by *ab initio* calculations

Experimental or theoretical (α_0)
Vibrational frequency analysis by spectrophotometry or electronic structure calculations

Theoretical (K_{BOELE})
Evaluation of $\delta E°$ due to adiabatic correction (diagonal nuclear motion correction)

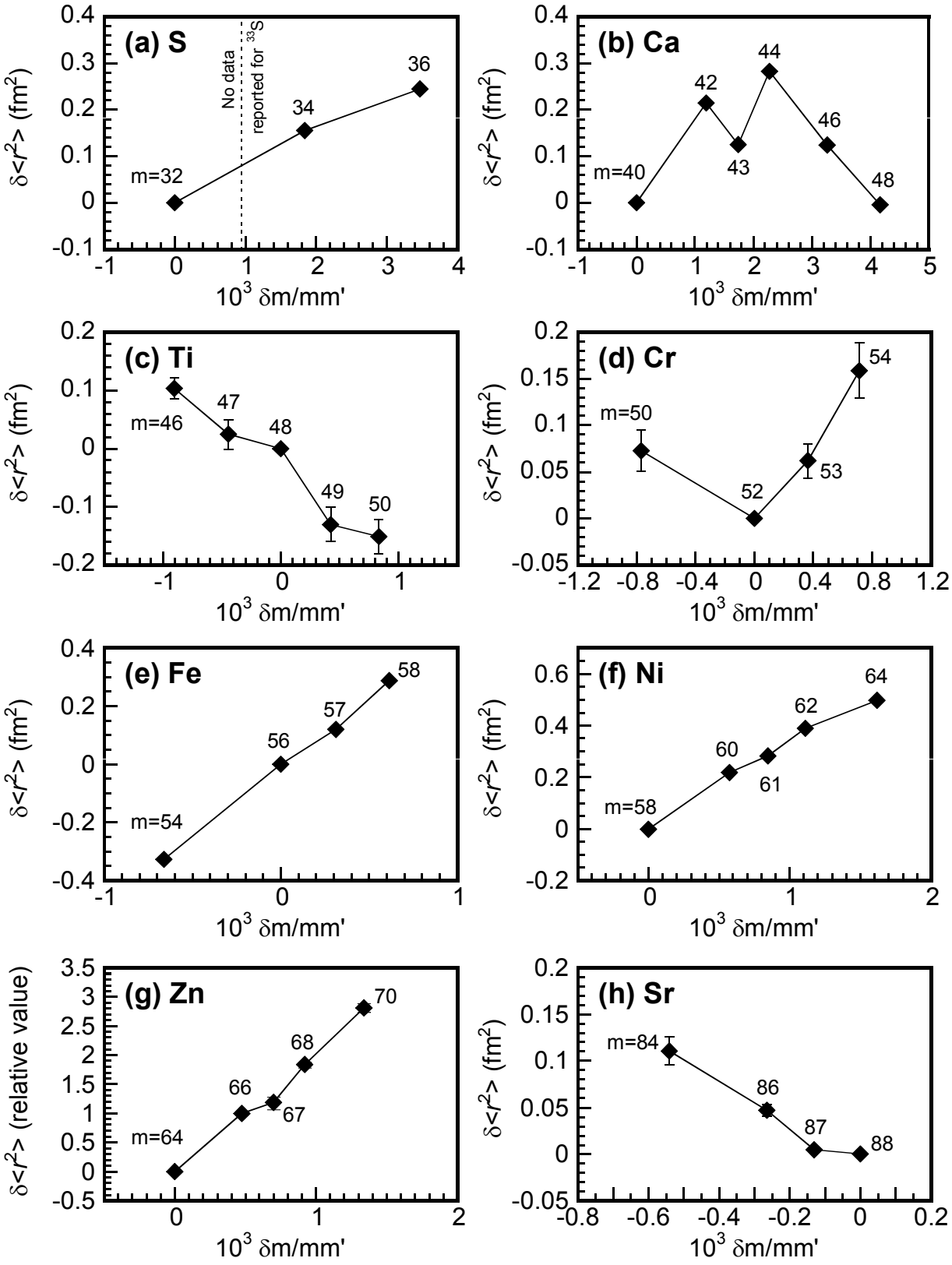
(a) S
No data reported for ^{33}S
m=32
34
36
(b) Ca
m=40
42
43
44
46
48
(c) Ti
m=46
47
48
49
50
(d) Cr
m=50
52
53
54
(e) Fe
m=54
56
57
58
(f) Ni
m=58
60
61
62
64
(g) Zn
m=64
66
67
68
70
(h) Sr
m=84
86
87
88
$\delta\langle r^2\rangle$ (fm^2)
$\delta\langle r^2\rangle$ (relative value)
10^3 δm/mm'

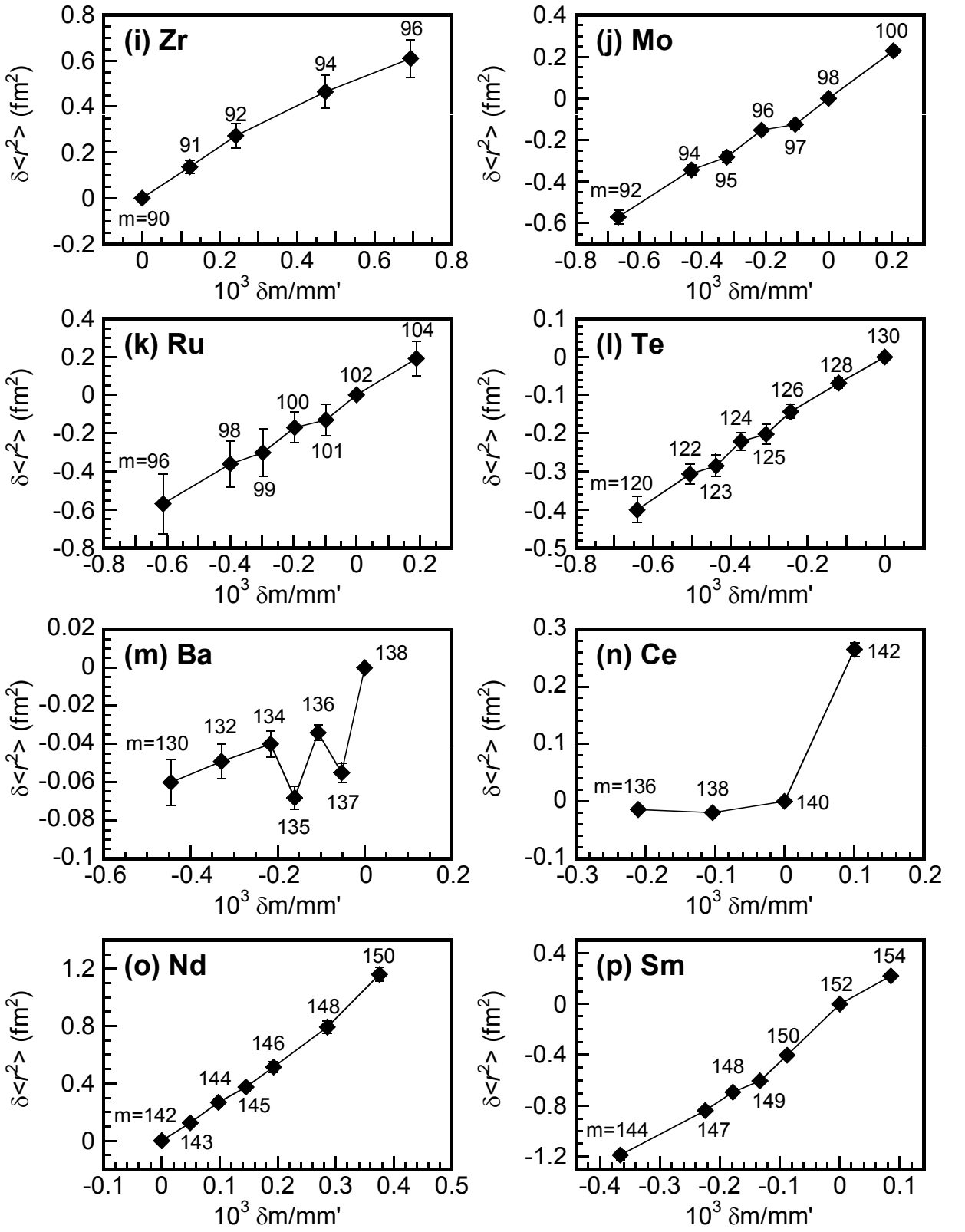
(i) Zr
m=90
91
92
94
96
(j) Mo
m=92
94
95
96
97
98
100
(k) Ru
m=96
98
99
100
101
102
104
(l) Te
m=120
122
123
124
125
126
128
130
(m) Ba
m=130
132
134
135
136
137
138
(n) Ce
m=136
138
140
142
(o) Nd
m=142
143
144
145
146
148
150
(p) Sm
m=144
147
148
149
150
152
154
δ<r²> (fm²)
10³ δm/mm'

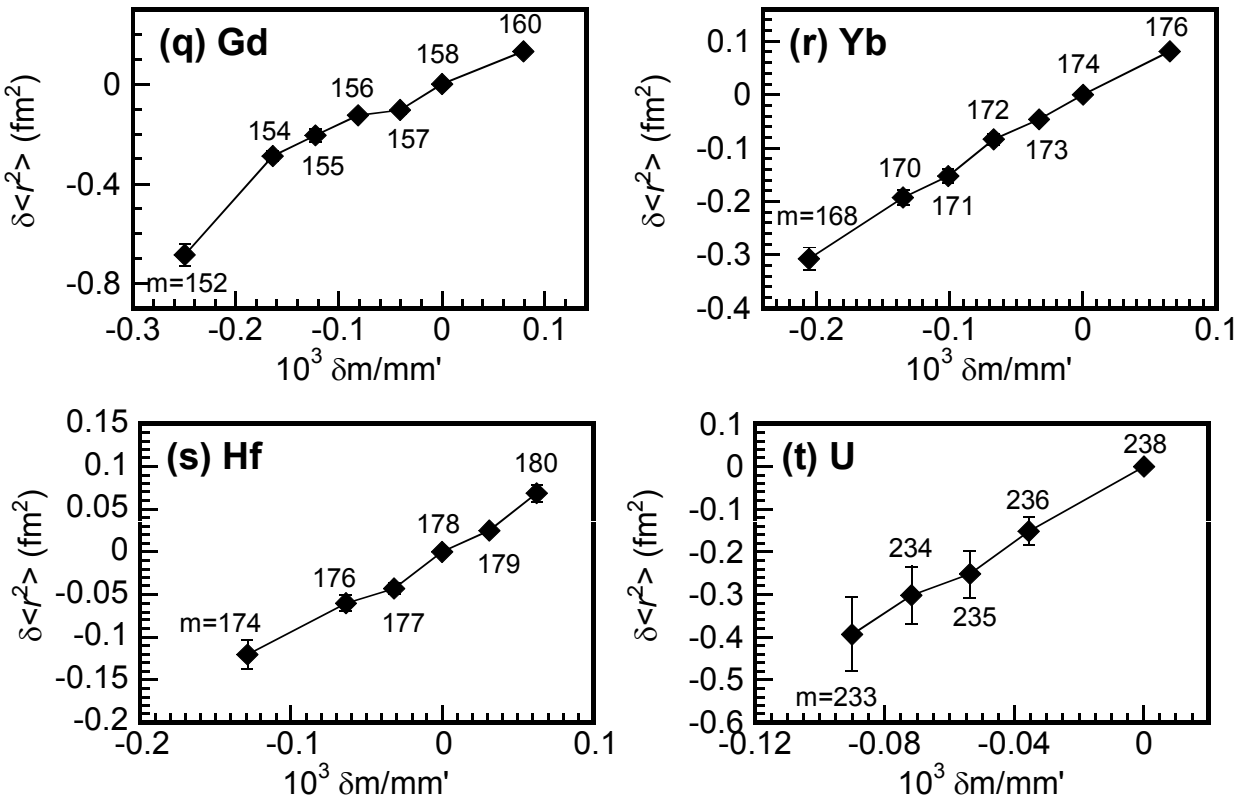
(q) Gd
(r) Yb
(s) Hf
(t) U
δ<r²> (fm²)
10³ δm/mm'
m=152
m=168
m=174
m=233
154
155
156
157
158
160
170
171
172
173
174
176
176
177
178
179
180
234
235
236
238

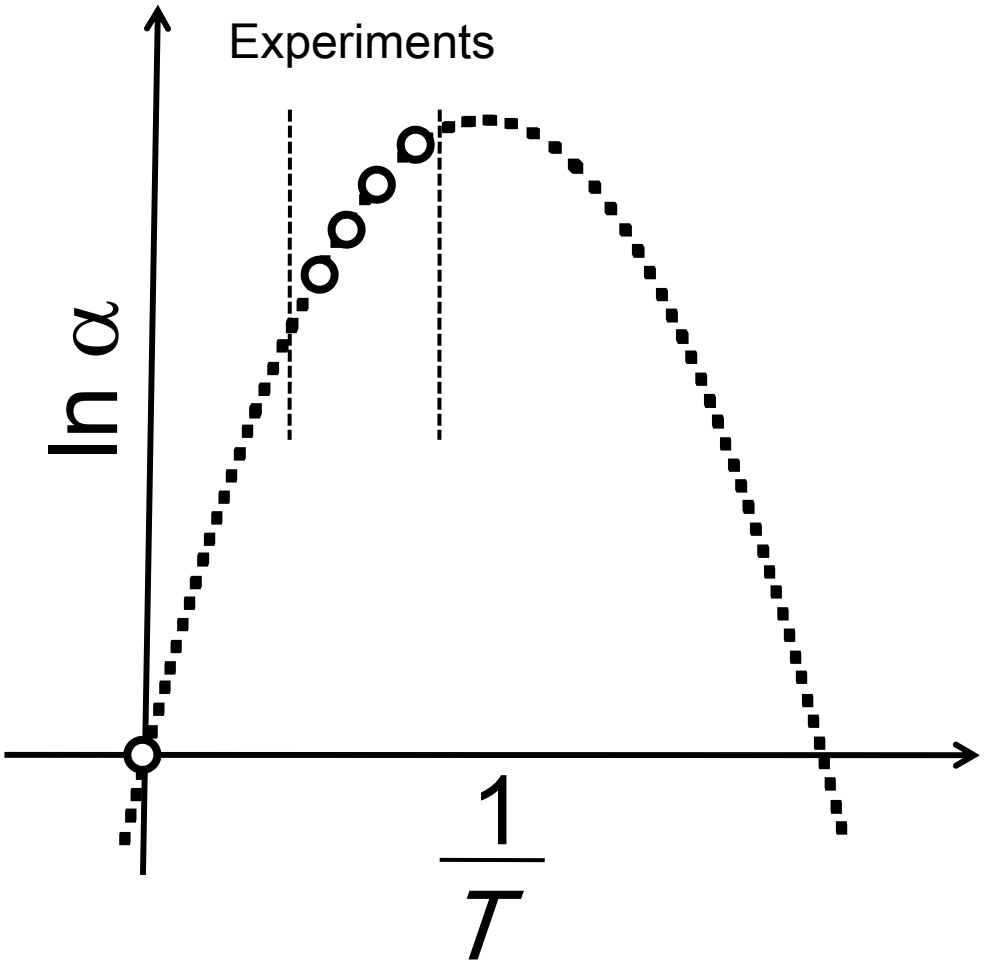

$$\ln \alpha = \frac{1}{T} C + \frac{1}{T^2} D$$

$$AX + Y \rightleftharpoons (AXY)^{\neq} \rightarrow AY + X$$

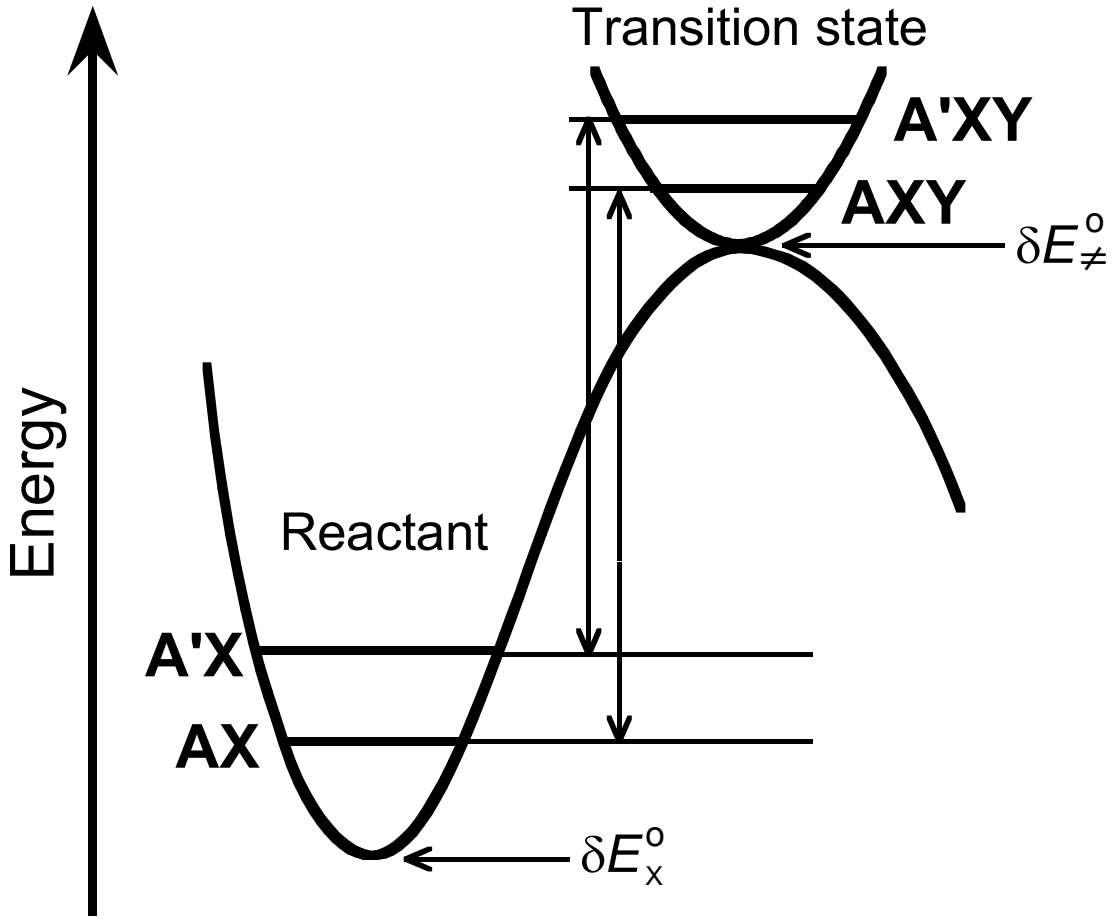

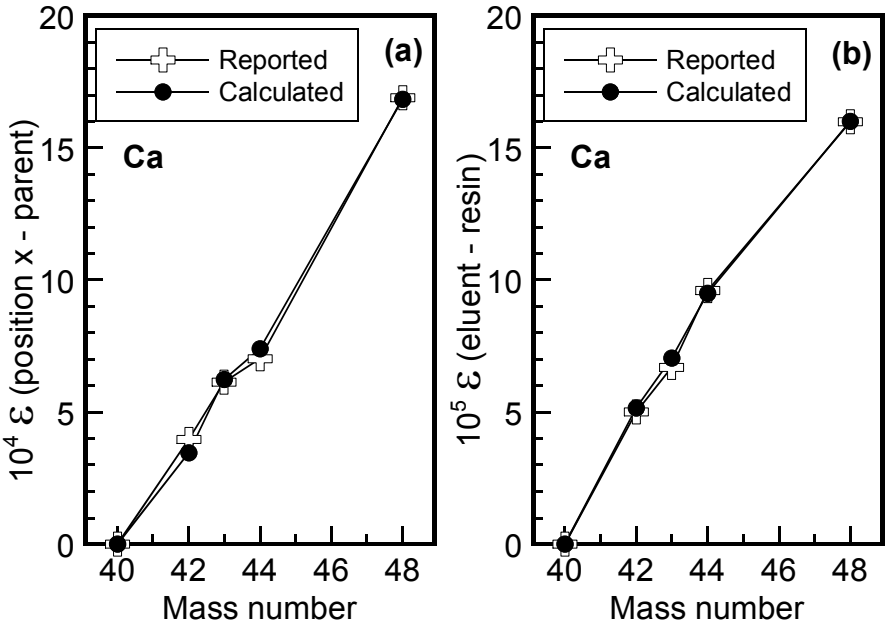
20
15
10
5
0
40
42
44
46
48
Mass number
10^4 ε (position x - parent)
Reported
Calculated
(a)
Ca
10^5 ε (eluent - resin)
(b)

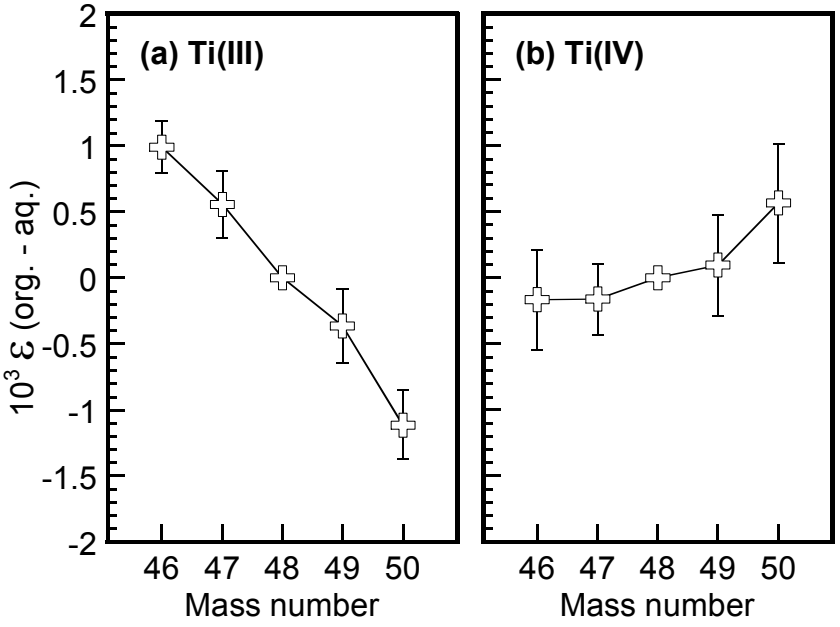
(a) Ti(III)
(b) Ti(IV)
10^3 ε (org. - aq.)
2
1.5
1
0.5
0
-0.5
-1
-1.5
-2
46 47 48 49 50
Mass number
46 47 48 49 50
Mass number

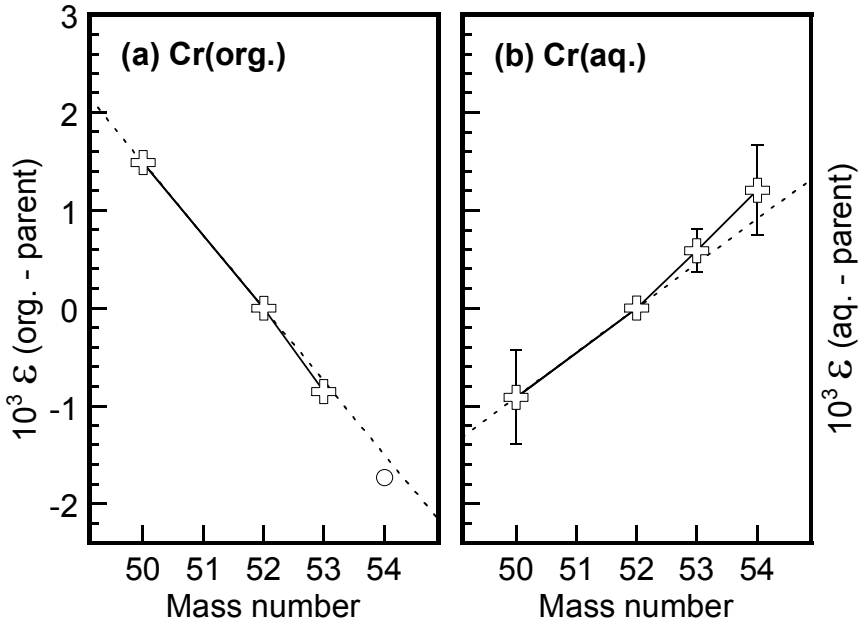
(a) Cr(org.)
(b) Cr(aq.)
3
2
1
0
-1
-2
10^3 ε (org. - parent)
10^3 ε (aq. - parent)
50 51 52 53 54
Mass number
50 51 52 53 54
Mass number

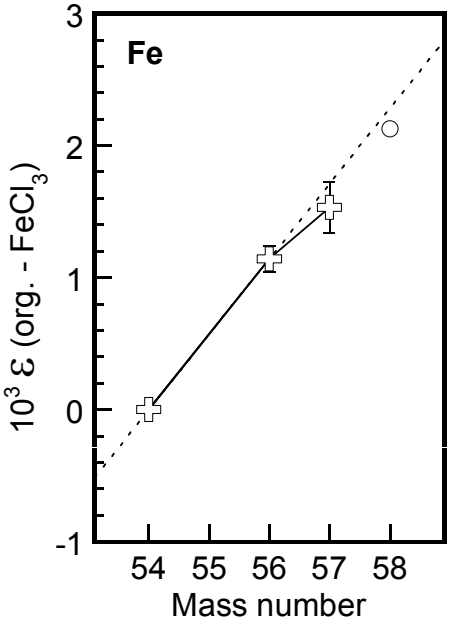
Fe
3
2
1
0
-1
10^3 ε (org. - $FeCl_3$)
54
55
56
57
58
Mass number

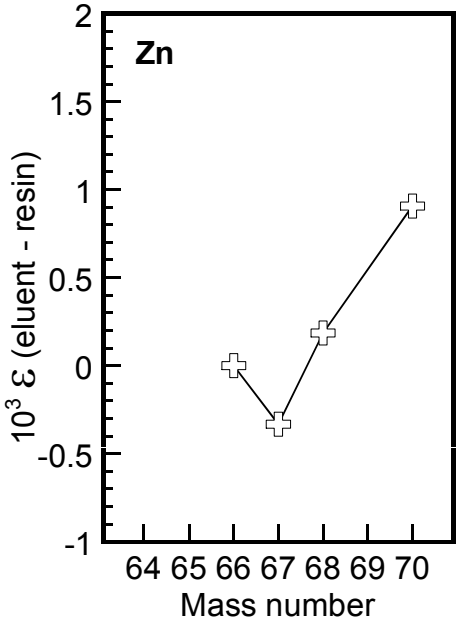
Zn
2
1.5
1
0.5
0
-0.5
-1
10^3 ε (eluent - resin)
64 65 66 67 68 69 70
Mass number

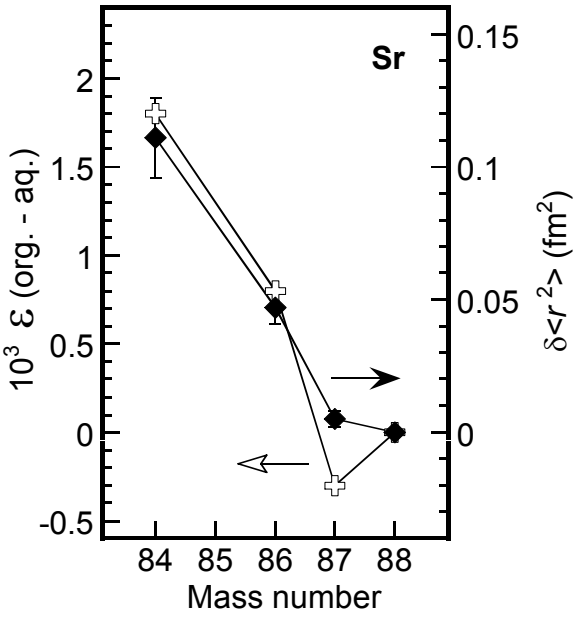
Sr
2
1.5
1
0.5
0
-0.5
0.15
0.1
0.05
0
84
85
86
87
88
Mass number
10^3 ε (org. - aq.)
δ<r^2> (fm^2)

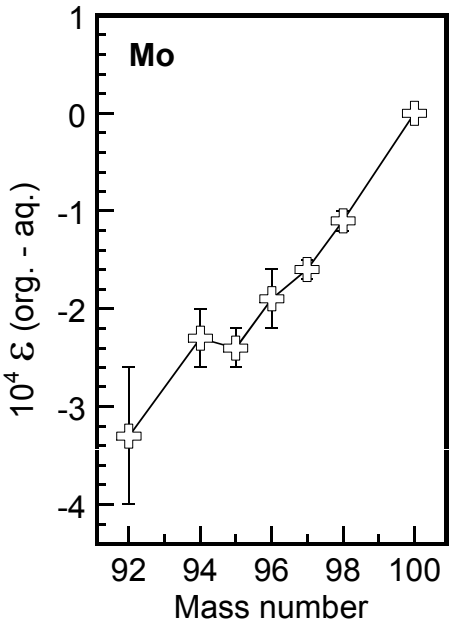
Mo
1
0
-1
-2
-3
-4
10^4 ε (org. - aq.)
92
94
96
98
100
Mass number

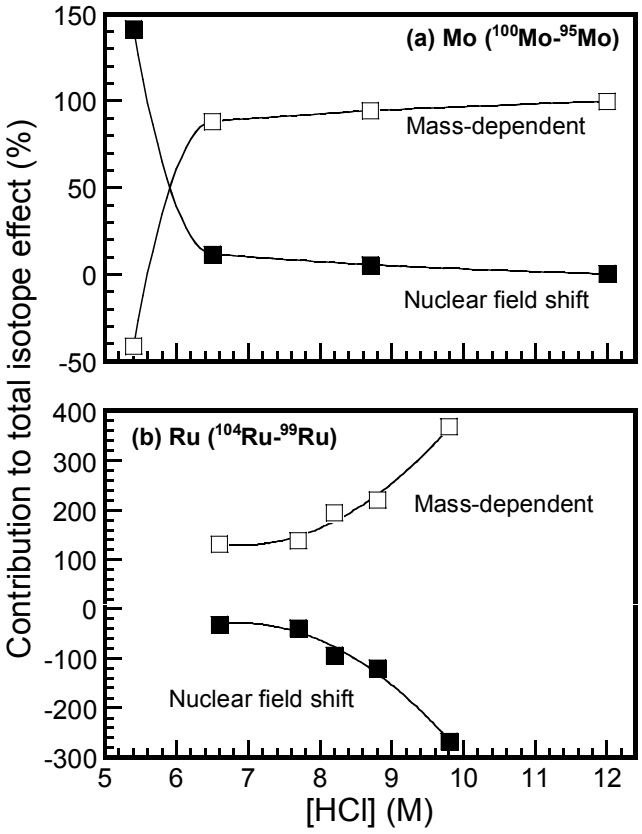
(a) Mo (^{100}Mo-^{95}Mo)
Mass-dependent
Nuclear field shift
(b) Ru (^{104}Ru-^{99}Ru)
Mass-dependent
Nuclear field shift
Contribution to total isotope effect (%)
[HCl] (M)
150
100
50
0
-50
400
300
200
100
0
-100
-200
-300
5
6
7
8
9
10
11
12

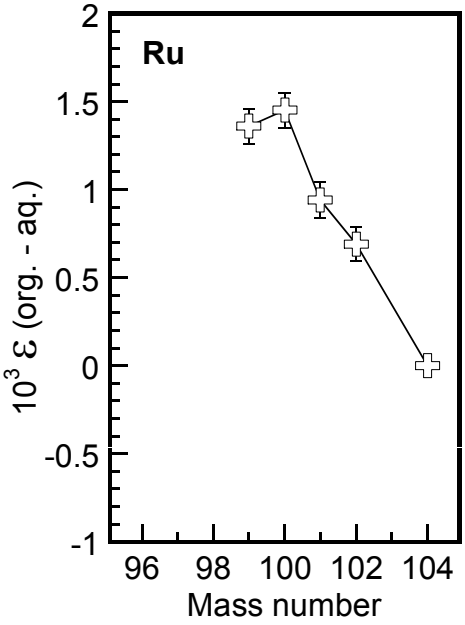
Ru
2
1.5
1
0.5
0
-0.5
-1
96
98
100
102
104
Mass number
10^3 ε (org. - aq.)

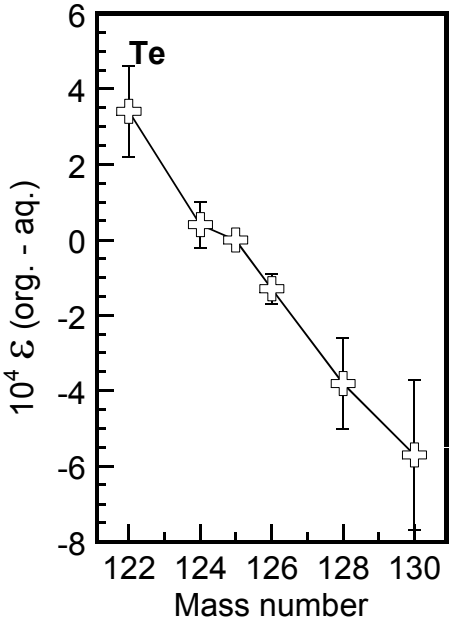
Te
6
4
2
0
-2
-4
-6
-8
122
124
126
128
130
Mass number
10^4 ε (org. - aq.)

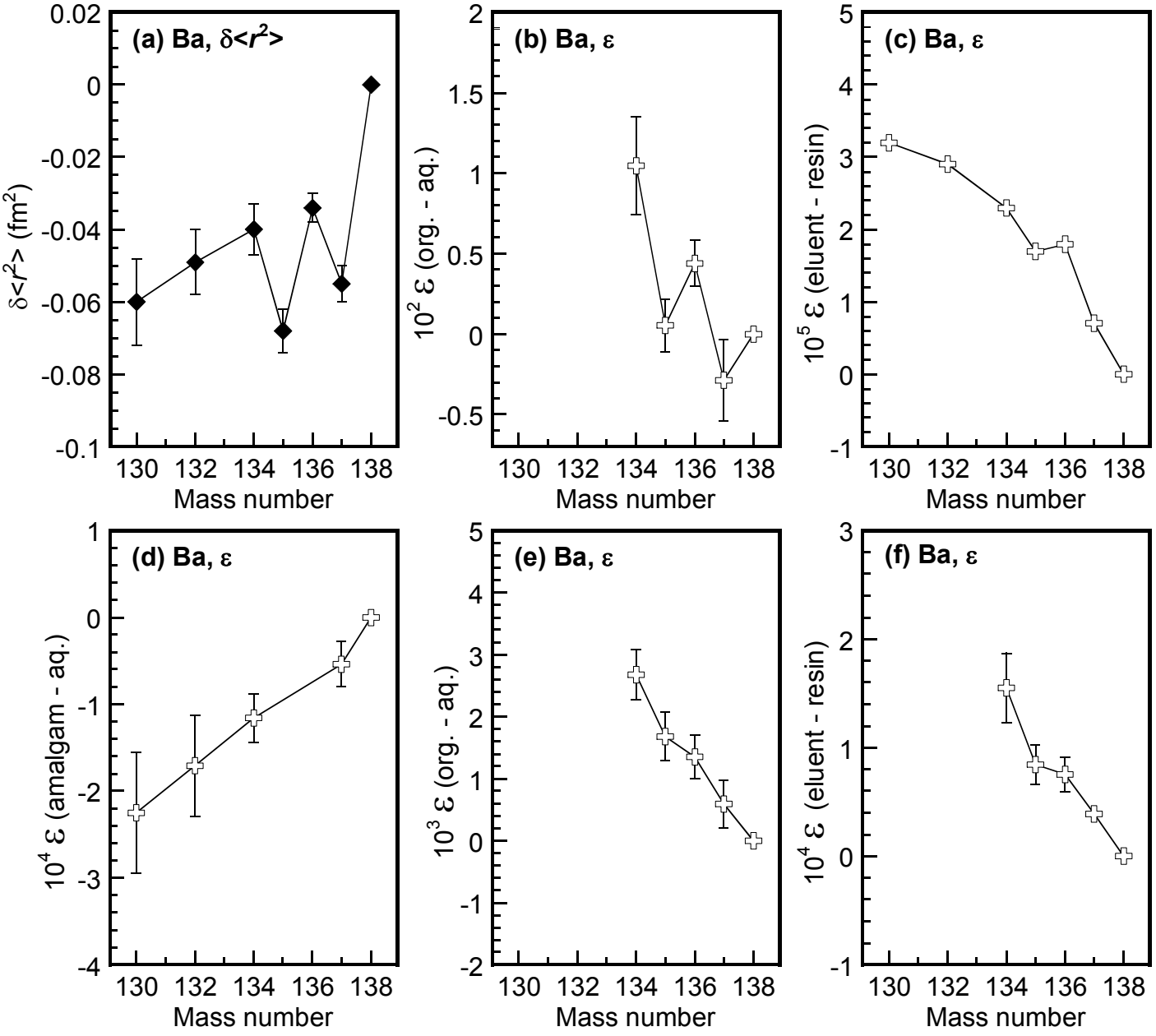
(a) Ba, δ<r²>
δ<r²> (fm²)
0.02
0
-0.02
-0.04
-0.06
-0.08
-0.1
130 132 134 136 138
Mass number
(b) Ba, ε
10² ε (org. - aq.)
2
1.5
1
0.5
0
-0.5
130 132 134 136 138
Mass number
(c) Ba, ε
10⁵ ε (eluent - resin)
5
4
3
2
1
0
-1
130 132 134 136 138
Mass number
(d) Ba, ε
10⁴ ε (amalgam - aq.)
1
0
-1
-2
-3
-4
130 132 134 136 138
Mass number
(e) Ba, ε
10³ ε (org. - aq.)
5
4
3
2
1
0
-1
-2
130 132 134 136 138
Mass number
(f) Ba, ε
10⁴ ε (eluent - resin)
3
2
1
0
-1
130 132 134 136 138
Mass number

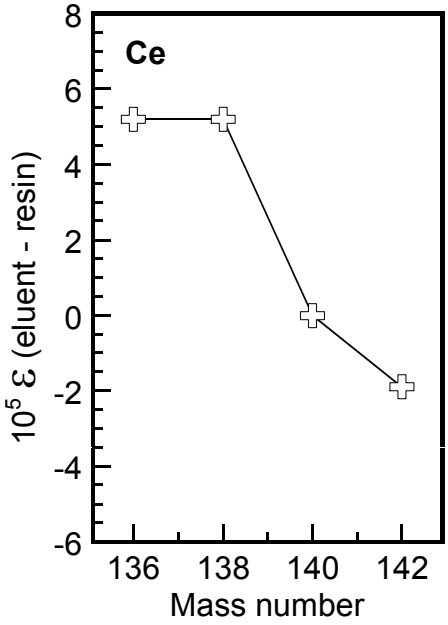
Ce
8
6
4
2
0
-2
-4
-6
136
138
140
142
Mass number
$10^5\ \varepsilon$ (eluent - resin)

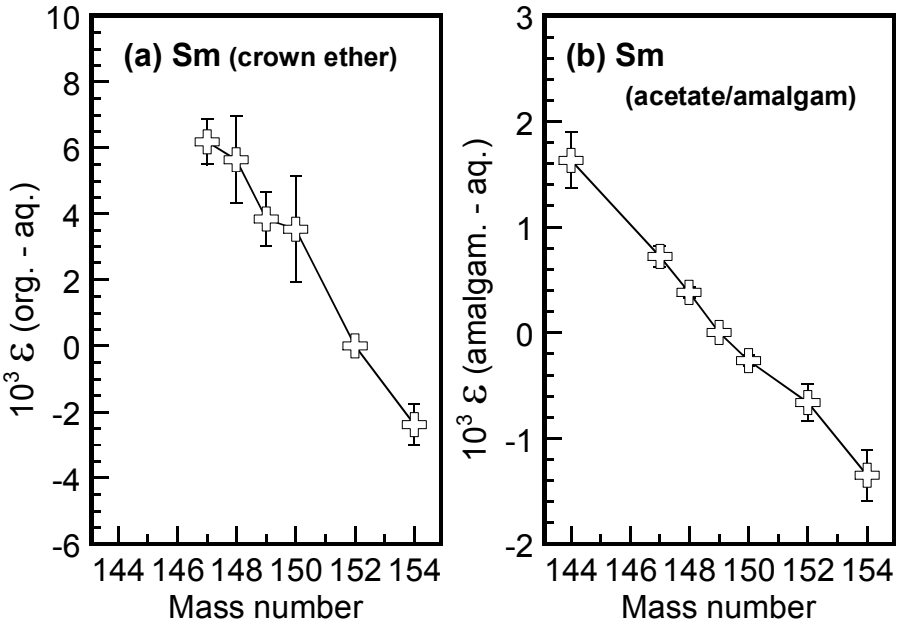
(a) Sm (crown ether)
10
8
6
4
2
0
-2
-4
-6
10^3 ε (org. - aq.)
144 146 148 150 152 154
Mass number
(b) Sm
(acetate/amalgam)
3
2
1
0
-1
-2
10^3 ε (amalgam. - aq.)
144 146 148 150 152 154
Mass number

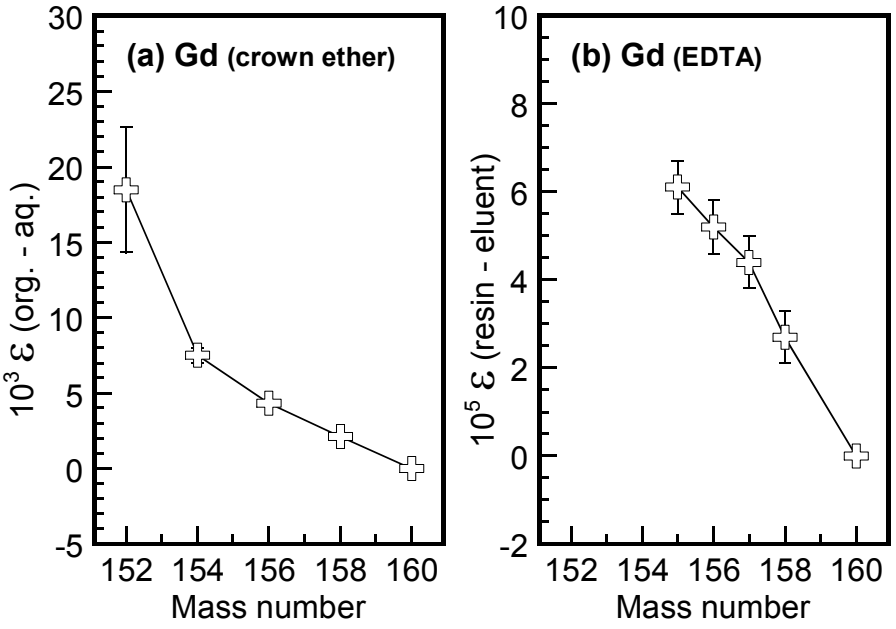
(a) Gd (crown ether)
10^3 ε (org. - aq.)
30
25
20
15
10
5
0
-5
152
154
156
158
160
Mass number
(b) Gd (EDTA)
10^5 ε (resin - eluent)
10
8
6
4
2
0
-2
152
154
156
158
160
Mass number

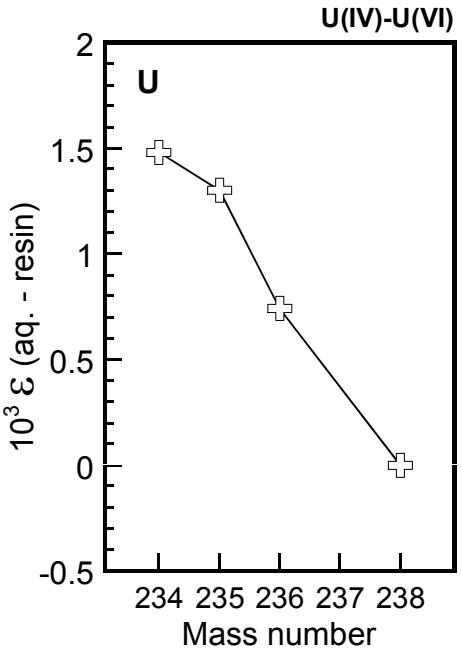
U(IV)-U(VI)
U
2
1.5
1
0.5
0
-0.5
10^3 ε (aq. - resin)
234 235 236 237 238
Mass number